

NODAL AUXILIARY SPACE PRECONDITIONING IN $\mathbf{H}(\mathbf{curl})$ AND $\mathbf{H}(\mathbf{div})$ SPACES*

RALF HIPTMAIR[†] AND JINCHAO XU[‡]

Abstract. In this paper, we develop and analyze a general approach to preconditioning linear systems of equations arising from conforming finite element discretizations of $\mathbf{H}(\mathbf{curl}, \Omega)$ - and $\mathbf{H}(\mathbf{div}, \Omega)$ -elliptic variational problems. The preconditioners exclusively rely on solvers for discrete Poisson problems. We prove mesh-independent effectivity of the preconditioners by using the abstract theory of auxiliary space preconditioning. The main tools are discrete analogues of so-called regular decomposition results in the function spaces $\mathbf{H}(\mathbf{curl}, \Omega)$ and $\mathbf{H}(\mathbf{div}, \Omega)$. Our preconditioner for $\mathbf{H}(\mathbf{curl}, \Omega)$ is similar to an algorithm proposed in [R. Beck, *Algebraic Multigrid by Component Splitting for Edge Elements on Simplicial Triangulations*, Tech. rep. SC 99-40, ZIB, Berlin, Germany, 1999].

Key words. auxiliary space preconditioning, fictitious space preconditioning, $\mathbf{H}(\mathbf{curl})$ and $\mathbf{H}(\mathbf{div})$, edge and face finite elements, algebraic multigrid

AMS subject classifications. 65N22, 65F10, 65N30, 65N55

DOI. 10.1137/060660588

1. Introduction. On a polyhedron Ω , scaled such that $\text{diam}(\Omega) = 1$, we consider the variational problems

$$(1.1) \quad \mathbf{u} \in \mathcal{H}(\mathbf{curl}) : \quad (\mathbf{curl} \mathbf{u}, \mathbf{curl} \mathbf{v})_0 + \tau (\mathbf{u}, \mathbf{v})_0 = (\mathbf{f}, \mathbf{v})_0 \quad \forall \mathbf{v} \in \mathcal{H}(\mathbf{curl}, \Omega),$$

$$(1.2) \quad \mathbf{u} \in \mathcal{H}(\mathbf{div}) : \quad (\mathbf{div} \mathbf{u}, \mathbf{div} \mathbf{v})_0 + \tau (\mathbf{u}, \mathbf{v})_0 = (\mathbf{f}, \mathbf{v})_0 \quad \forall \mathbf{v} \in \mathcal{H}(\mathbf{div}, \Omega),$$

where \mathbf{f} is a vector field in $(L^2(\Omega))^3$ and $\tau \geq 0$. We admit both homogeneous natural and essential boundary conditions; that is, $\mathcal{H}(\mathbf{div}, \Omega)$ and $\mathcal{H}(\mathbf{curl}, \Omega)$ can stand for either $\mathbf{H}(\mathbf{curl}, \Omega)$ and $\mathbf{H}(\mathbf{div}, \Omega)$ or $\mathbf{H}_0(\mathbf{curl}, \Omega)$ and $\mathbf{H}_0(\mathbf{div}, \Omega)$, respectively. The parameter τ controls the relative weight of the second and zero order terms in the bilinear forms.

More generally, the bilinear forms of (1.1) and (1.2) could feature spatially varying coefficients. So far, our theoretical analysis can take into account variations in the coefficients only very crudely. Thus, for the sake of simplicity, we have decided to focus on the constant coefficient case. Variable coefficients will be covered in some numerical experiments.

Variational problems of the form (1.1) and (1.2) arise in different applications, for instance, in

- (1.1) as a variational formulation of the eddy current model in computational electromagnetics [9], and
- (1.2) in the context of equivalent operator preconditioning for mixed finite element and first order system least squares (FOSLS) schemes for second order elliptic problems [3].

*Received by the editors May 23, 2006; accepted for publication (in revised form) May 7, 2007; published electronically November 28, 2007.

<http://www.siam.org/journals/sinum/45-6/66058.html>

[†]Seminar for Applied Mathematics, ETH Zürich, CH-8092 Zürich, Switzerland (hiptmair@sam.math.ethz.ch).

[‡]Mathematics Department, The Pennsylvania State University, University Park, PA 16802 (xu@math.psu.edu).

Geometric multigrid approaches to discrete linear problems arising from the Galerkin finite element discretization of (1.1) and (1.2) are well known [2, 4, 19, 22]. They supply mesh-independent iterative solvers and preconditioners, provided a hierarchy of uniformly shape regular meshes is available. Algebraic multigrid (AMG) methods that dispense with this requirement have been proposed in [7, 33], but they noticeably deteriorate on fine meshes, let alone permit a comprehensive theoretical analysis. The auxiliary space approach [38] allows us to harness powerful and asymptotically optimal AMG methods developed for discrete second order elliptic boundary value problems in order to get fast iterative solvers for discretized $\mathbf{H}(\mathbf{curl}, \Omega)$ - and $\mathbf{H}(\mathbf{div}, \Omega)$ -elliptic problems. As these auxiliary discrete second order elliptic boundary value problems arise from the use of Lagrangian finite elements, which are known as nodal finite elements in computational electromagnetism [10], we have tagged this special auxiliary space technique as *nodal*.

There is a close relationship between the variational problems (1.1) and (1.2) (cf. [20, section 2]) which allows a fairly parallel treatment of both. Thus we opt for a unified presentation, starting from an abstract variational problem

$$(1.3) \quad \mathbf{u} \in \mathcal{H}(\mathbf{D}, \Omega) : \quad a(\mathbf{u}, \mathbf{v}) := (\mathbf{D}\mathbf{u}, \mathbf{D}\mathbf{v})_0 + \tau(\mathbf{u}, \mathbf{v})_0 = f(\mathbf{v}) \quad \forall \mathbf{u}, \mathbf{v} \in \mathcal{H}(\mathbf{D}, \Omega),$$

where f is a continuous linear functional on the Hilbert space $\mathcal{H}(\mathbf{D}, \Omega)$. Relating (1.3) to (1.1) and (1.2) discloses the meaning of \mathbf{D} , f , and $\mathcal{H}(\mathbf{D}, \Omega)$; see also Table 3.1. The bilinear form $a(\cdot, \cdot)$ induces the *energy norm*

$$(1.4) \quad \|\mathbf{v}\|_A^2 := a(\mathbf{v}, \mathbf{v}), \quad \mathbf{v} \in \mathcal{H}(\mathbf{D}, \Omega),$$

which is merely a seminorm, if $\tau = 0$. The energy norm is closely related to the Hilbert space norm on $\mathcal{H}(\mathbf{D}, \Omega)$

$$(1.5) \quad \|\mathbf{v}\|_{\mathcal{H}(\mathbf{D}, \Omega)}^2 := \|\mathbf{D}\mathbf{v}\|_{L^2(\Omega)}^2 + \|\mathbf{v}\|_{L^2(\Omega)}^2, \quad \mathbf{v} \in \mathcal{H}(\mathbf{D}, \Omega).$$

The principal challenge confronted in the development of preconditioners for discretized versions of (1.1) and (1.2) is the presence of a large kernel of \mathbf{D} : in contrast to the case $\mathbf{D} = \mathbf{grad}$, these kernels have infinite dimension for $\mathbf{D} = \mathbf{curl}$ (comprising, e.g., all gradients) and $\mathbf{D} = \mathbf{div}$ (comprising, e.g., all rotations). This entails a separate treatment of these kernels by the preconditioner, which can exploit the fact that in suitable \mathbf{curl} - and \mathbf{div} -conforming finite element spaces the kernels possess a convenient representation through potentials. On the complement of the kernel the variational problem should display strong ellipticity and be amenable to standard elliptic preconditioning techniques; cf. the reasoning in [19, section 3] and [5, section 5].

Roughly speaking, on the complement of the kernels, the differential operators underlying (1.1) and (1.2) can be expected to be spectrally equivalent to a second order differential operator applied to the components of the vector fields. However, using a discrete second order differential operator as preconditioner is not possible immediately, because it does not fit the \mathbf{curl} - and \mathbf{div} -conforming finite element space. This is why we need the auxiliary space preconditioning technology [38] to link the finite element spaces on which (1.3) is discretized and the vectorial $H^1(\Omega)$ -conforming finite elements that underlie the preconditioning operator.

The main rationale for pursuing this method in [5] was that the evaluation of the preconditioner boils down to inverting discrete scalar second order elliptic operators approximately. Fast AMG methods for this purpose abound; see [36, Appendix A]. Thus, AMG codes can be harnessed for $\mathbf{H}(\mathbf{curl}, \Omega)$ - and $\mathbf{H}(\mathbf{div}, \Omega)$ -elliptic problems.

The principal idea underlying our approach can be gleaned from the understanding that stable space decompositions are at the heart of preconditioners for symmetric positive definite variational problems; see section 2 for further explanations. Results that we have dubbed regular decompositions provide fundamental stable splittings for the spaces $\mathcal{H}(\mathbf{D}, \Omega)$; see section 3 for details. For instance, for the space $\mathbf{H}_0(\mathbf{curl}, \Omega)$ we have a stable splitting

$$\mathbf{H}_0(\mathbf{curl}, \Omega) = (H_0^1(\Omega))^3 + \mathbf{grad} H_0^1(\Omega).$$

This suggests that a preconditioner for $\mathbf{H}_0(\mathbf{curl}, \Omega)$ -elliptic variational problem can be based on solving $H_0^1(\Omega)$ -elliptic variational problems. However, to make this idea work, the splittings have to be adapted to the discrete setting. Thus, in sections 5 and 6 we establish stable discrete regular decompositions and corresponding norm equivalences. This yields the desired preconditioners, whose implementation will be discussed in section 7. In the end, we supplement the asymptotic theoretical estimate with numerical studies of the performance of the preconditioners. We refer the reader to [27, 28] for more numerical results.

2. Auxiliary space preconditioning: Abstract theory. In this section, we give a self-contained description of preconditioning techniques based on fictitious or auxiliary spaces as developed in [18, 31, 38].

Let V stand for a real Hilbert space with inner product $a(\cdot, \cdot)$ and (energy) norm $\|\cdot\|_A$. The fictitious space method targets linear variational problems

$$(2.1) \quad u \in V : \quad a(u, v) = f(v) \quad \forall v \in V.$$

Its main building blocks are

1. a *fictitious space* \bar{V} , that is, another real Hilbert space equipped with the inner product $\bar{a}(\cdot, \cdot)$, which induces the norm $\|\cdot\|_{\bar{A}}$, and
2. a continuous and surjective linear transfer operator $\Pi : \bar{V} \mapsto V$.

We tag dual spaces by $'$ and adjoint operators by $*$, and we use angle brackets for duality pairings. Then, writing $A : V \mapsto V'$ and $\bar{A} : \bar{V} \mapsto \bar{V}'$ for the isomorphisms associated with $a(\cdot, \cdot)$ and $\bar{a}(\cdot, \cdot)$, respectively, the fictitious space preconditioner is given by

$$(2.2) \quad B = \Pi \circ \bar{A}^{-1} \circ \Pi^* : V' \mapsto V.$$

Obviously, the operator B is associated with a symmetric bilinear form on the dual space V' . The next lemma confirms that this form is actually positive definite, which renders B a valid preconditioner.

LEMMA 2.1. *If $\Pi : \bar{V} \mapsto V$ is surjective, then the operator B is an isomorphism.*

Proof. Π being surjective means that it is an open mapping and Π^* is injective. As \bar{a} is positive definite, we infer

$$\langle \varphi, B\varphi \rangle_{V' \times V} = \langle \Pi^* \varphi, \bar{A}^{-1} \Pi^* \varphi \rangle_{\bar{V}' \times \bar{V}} > 0 \quad \forall \varphi \in V' \setminus \{0\}.$$

From this we conclude the assertion of the theorem. \square

The next theorem is known as the *fictitious space lemma* [31], for which we provide the elementary proof for the sake of completeness.

THEOREM 2.2 (fictitious space lemma). *Assume that Π is surjective and*

$$(2.3) \quad \exists c_0 > 0 : \quad \forall v \in V : \quad \exists \bar{v} \in \bar{V} : \quad v = \Pi \bar{v} \quad \wedge \quad \|\bar{v}\|_{\bar{A}} \leq c_0 \|v\|_A,$$

$$(2.4) \quad \exists c_1 > 0 : \quad \|\Pi \bar{v}\|_A \leq c_1 \|\bar{v}\|_{\bar{A}} \quad \forall \bar{v} \in \bar{V}.$$

Then

$$(2.5) \quad c_0^{-2} \|v\|_A^2 \leq a(\mathbf{B}Av, v) \leq c_1^2 \|v\|_A^2 \quad \forall v \in V.$$

Proof. The proof makes use of only the Cauchy–Schwarz inequality:

$$\begin{aligned} a(\mathbf{B}Av, v) &\leq a(\mathbf{B}Av, \mathbf{B}Av)^{1/2} a(v, v)^{1/2} \\ &= a(\Pi \bar{\mathbf{A}}^{-1} \Pi^* \mathbf{A}v, \Pi \bar{\mathbf{A}}^{-1} \Pi^* \mathbf{A}v)^{1/2} \|v\|_A \\ &\leq c_1 \bar{a}(\bar{\mathbf{A}}^{-1} \Pi^* \mathbf{A}v, \bar{\mathbf{A}}^{-1} \Pi^* \mathbf{A}v)^{1/2} \|v\|_A \\ &= c_1 \langle \Pi^* \mathbf{A}v, \bar{\mathbf{A}}^{-1} \Pi^* \mathbf{A}v \rangle_{\bar{V}' \times \bar{V}}^{1/2} \|v\|_A = c_1 a(\mathbf{B}Av, v)^{1/2} \|v\|_A. \end{aligned}$$

Next, we rely on the assumption (2.3) and get

$$\begin{aligned} a(v, v) &= \langle Av, \Pi \bar{v} \rangle_{V' \times V} = \langle \Pi^* \mathbf{A}v, \bar{v} \rangle_{\bar{V}' \times \bar{V}} = \bar{a}(\bar{\mathbf{A}}^{-1} \Pi^* \mathbf{A}v, \bar{v}) \\ &\leq \bar{a}(\bar{\mathbf{A}}^{-1} \Pi^* \mathbf{A}v, \bar{\mathbf{A}}^{-1} \Pi^* \mathbf{A}v)^{1/2} \|\bar{v}\|_{\bar{\mathbf{A}}} \leq c_0 a(\mathbf{B}Av, v)^{1/2} \|v\|_A. \quad \square \end{aligned}$$

From (2.5) we immediately get an estimate for the spectral condition number of the preconditioned operator \mathbf{A} :

$$(2.6) \quad \kappa(\mathbf{B}\mathbf{A}) := \frac{\lambda_{\max}(\mathbf{B}\mathbf{A})}{\lambda_{\min}(\mathbf{B}\mathbf{A})} \leq (c_0 c_1)^2.$$

COROLLARY 2.3. *Under the assumptions of the previous theorem, we have the following estimate for the spectral condition number:*

$$\kappa((\Pi \bar{\mathbf{B}} \Pi^*) \mathbf{A}) \leq \kappa(\bar{\mathbf{B}} \bar{\mathbf{A}}) (c_0 c_1)^2,$$

where $\bar{\mathbf{B}} : \bar{V}' \mapsto \bar{V}$ is supposed to be a preconditioner for $\bar{\mathbf{A}}$.

Proof. This result is a consequence of the obvious inequality

$$\kappa((\Pi \bar{\mathbf{B}} \Pi^*) \mathbf{A}) \leq \kappa(\bar{\mathbf{B}} \bar{\mathbf{A}}) \kappa(\mathbf{B}\mathbf{A}). \quad \square$$

The auxiliary space method as pioneered in [38] can be viewed as a fictitious space approach relying on the special choice

$$(2.7) \quad \bar{V} = V \times W_1 \times \cdots \times W_J,$$

where W_1, \dots, W_J , $J \in \mathbb{N}$, are Hilbert spaces endowed with inner products $\bar{a}_j(\cdot, \cdot)$, $j = 1, \dots, J$. They provide the so-called auxiliary spaces.

A distinctive feature of the auxiliary space method is the presence of V in (2.7), but as a component of \bar{V} the space V will be equipped with an inner product $s(\cdot, \cdot)$ different from $a(\cdot, \cdot)$. The operator $\mathbf{S} : V \mapsto V'$ induced by $s(\cdot, \cdot)$ on V is usually called the *smoother*. In other words, the auxiliary space method adopts the fictitious space approach with the inner product

$$(2.8) \quad \bar{a}(\bar{v}, \bar{v}) := s(v_0, v_0) + \sum_{j=1}^J \bar{a}_j(w_j, w_j), \quad \begin{aligned} \bar{v} &= (v_0, w_1, \dots, w_J) \in \bar{V}, \\ v_0 &\in V, w_j \in W_j. \end{aligned}$$

Furthermore, for each W_j we need a linear transfer operator $\Pi_j : W_j \mapsto V$, from which we build the surjective operator

$$(2.9) \quad \Pi := \begin{pmatrix} Id & & & \\ & \Pi_1 & & \\ & & \ddots & \\ & & & \Pi_J \end{pmatrix} : \bar{V} \mapsto V.$$

Now, all components of the auxiliary space preconditioner are in place and the formula (2.2) becomes

$$(2.10) \quad \mathbf{B} = \mathbf{S}^{-1} + \sum_{j=1}^J \Pi_j \circ \bar{\mathbf{A}}_j^{-1} \circ \Pi_j^*.$$

The verification of the assumptions of Theorem 2.2 for the preconditioner boils down to three steps.

1. Find bounds $c_j > 0$ for norms of the transfer operators Π_j :

$$(2.11) \quad \|\Pi_j w_j\|_A \leq c_j \bar{a}(w_j, w_j)^{1/2}, \quad w_j \in W_j.$$

2. Investigate the continuity of \mathbf{S}^{-1} :

$$(2.12) \quad \exists c_s > 0 : \quad \|v\|_A \leq c_s s(v, v)^{1/2} \quad \forall v \in V.$$

3. Establish that for every $v \in V$ there are $v_0 \in V$ and $w_j \in W_j$ such that $v = v_0 + \sum_{j=1}^J \Pi_j w_j$ and

$$(2.13) \quad s(v_0, v_0) + \sum_{j=1}^J \bar{a}_j(w_j, w_j) \leq c_0^2 \|v\|_A^2,$$

where $c_0 > 0$ should be small and independent of v .

Then, the assertion of Theorem 2.2 translates to

$$(2.14) \quad \kappa(\mathbf{BA}) \leq c_0^2 (c_s^2 + c_1^2 + \cdots + c_J^2).$$

It goes without saying that in the spirit of Corollary 2.3, the bilinear forms \bar{a}_j on the auxiliary spaces W_j can be replaced with spectrally equivalent bilinear forms \bar{b}_j ; i.e., we may use preconditioners $\bar{\mathbf{B}}_j$ for the operators $\bar{\mathbf{A}}_j$. The impact of this approximation can be gauged as in Corollary 2.3.

In the applications we have in mind all the spaces will be finite element spaces and will feature bases comprised of locally supported functions. Plugging basis functions into the bilinear forms $a(\cdot, \cdot)$ and $\bar{a}_j(\cdot, \cdot)$, we obtain the Galerkin matrices $\mathbf{A} \in \mathbb{R}^{N, N}$, $N := \dim V$, $\bar{\mathbf{A}}_j \in \mathbb{R}^{N_j, N_j}$, $N_j := \dim W_j$. The smoother is provided by local relaxation procedures: for instance, if Jacobi smoothing is used, an algebraic representation of the associated operator \mathbf{S} is given by the diagonal part \mathbf{D}_A of the matrix \mathbf{A} . Hence, the algebraic version of the preconditioner from (2.10) reads

$$(2.15) \quad \mathbf{B} = \mathbf{D}_A^{-1} + \sum_{j=1}^J \mathbf{P}_j \bar{\mathbf{A}}_j^{-1} \mathbf{P}_j^T,$$

where $\mathbf{P}_j \in \mathbb{R}^{N, N_j}$ is the matrix representation of Π_j . When using symmetric Gauss–Seidel smoothing \mathbf{D}_A^{-1} has to be replaced with $\mathbf{L}_A^{-1} + \mathbf{L}_A^{-T} - \mathbf{L}_A^{-1} \mathbf{A} \mathbf{L}_A^{-T}$, where \mathbf{L}_A stands for the lower triangular part of (the symmetric matrix) \mathbf{A} .

Remark 1. Naturally, we can also try to apply the successive subspace correction idea [37] to the multiple auxiliary spaces to obtain the following iterative method for the operator equation $Au = f$, $f \in V'$:

$$(2.16) \quad u \leftarrow u + \mathbf{S}^{-1}(f - Au), \quad u \leftarrow u + \Pi_j \bar{\mathbf{B}}_j \Pi_j^*(f - Au), \quad 1 \leq j \leq J.$$

It is easy to see that a sufficient condition for the convergence of this successive auxiliary space method is

$$(2.17) \quad \lambda_{\max}(\bar{\mathbf{B}}_j \bar{\mathbf{A}}_j) \leq \frac{\omega}{c_j}, \quad 1 \leq j \leq J,$$

for some $0 < \omega < 2$. Under the above conditions, the convergence rate of the iteration (2.16) depends only on c_0 , c_s , c_j ($1 \leq j \leq J$), ω , and J .

3. Regular decompositions. The abstract theory of the previous section has identified the uniform stability of decompositions (cf. (2.13)) as a key prerequisite of successful auxiliary space preconditioning. This connects well with the pivotal role of certain stable decomposition in the analysis of variational problems linked with $\mathbf{H}(\mathbf{curl}, \Omega)$ and $\mathbf{H}(\mathbf{div}, \Omega)$ [6, 12, 14]. In the subsequent discussion, to avoid topological obstructions, we restrict ourselves to “simple” domains.

ASSUMPTION 3.1. *We assume that Ω is homotopy equivalent to a ball.*

This makes it possible to use *potential representations* for the kernels of the differential operators.

LEMMA 3.1 (exact sequence property).

$$\begin{aligned} \text{Assumption 3.1} \quad \Rightarrow \quad & \mathbf{H}(\mathbf{curl} 0, \Omega) := \{\mathbf{v} \in \mathbf{H}(\mathbf{curl}, \Omega) : \mathbf{curl} \mathbf{v} = 0\} = \mathbf{grad} H^1(\Omega), \\ & \mathbf{H}_0(\mathbf{curl} 0, \Omega) := \{\mathbf{v} \in \mathbf{H}_0(\mathbf{curl}, \Omega) : \mathbf{curl} \mathbf{v} = 0\} = \mathbf{grad} H_0^1(\Omega), \\ & \mathbf{H}(\mathbf{div} 0, \Omega) := \{\mathbf{v} \in \mathbf{H}(\mathbf{div}, \Omega) : \mathbf{div} \mathbf{v} = 0\} = \mathbf{curl} \mathbf{H}(\mathbf{curl}, \Omega), \\ & \mathbf{H}_0(\mathbf{div} 0, \Omega) := \{\mathbf{v} \in \mathbf{H}_0(\mathbf{div}, \Omega) : \mathbf{div} \mathbf{v} = 0\} = \mathbf{curl} \mathbf{H}_0(\mathbf{curl}, \Omega). \end{aligned}$$

In the unifying framework, this lemma can be recast into

$$(3.1) \quad \text{Assumption 3.1} \quad \Rightarrow \quad \mathcal{H}(\mathbf{D}0, \Omega) := \{\mathbf{v} \in \mathcal{H}(\mathbf{D}, \Omega) : \mathbf{D}\mathbf{v} = 0\} = \mathbf{D}^- \mathcal{H}(\mathbf{D}^-, \Omega),$$

where \mathbf{D}^- is the differential operator characterizing the *potential* space $\mathcal{H}(\mathbf{D}^-, \Omega)$; see the “translation table” Table 3.1.

TABLE 3.1
Translation table for unifying notational framework, generic case.

D	$\mathcal{H}(\mathbf{D}, \Omega)$	\mathbf{D}^-	$\mathcal{H}(\mathbf{D}^-, \Omega)$	\mathbf{D}^+	\mathcal{H}^1
grad	$H^1(\Omega)$ $H_0^1(\Omega)$	<i>Id</i>	$\{\text{const}\}$ $\{0\}$	curl	$H^1(\Omega)$ $H_0^1(\Omega)$
curl	$\mathbf{H}(\mathbf{curl}, \Omega)$ $\mathbf{H}_0(\mathbf{curl}, \Omega)$	grad	$H^1(\Omega)$ $H_0^1(\Omega)$	div	$(H^1(\Omega))^3$ $(H_0^1(\Omega))^3$
div	$\mathbf{H}(\mathbf{div}, \Omega)$ $\mathbf{H}_0(\mathbf{div}, \Omega)$	curl	$\mathbf{H}(\mathbf{curl}, \Omega)$ $\mathbf{H}_0(\mathbf{curl}, \Omega)$	0	$(H^1(\Omega))^3$ $(H_0^1(\Omega))^3$

Remark 2. If Assumption 3.1 fails to hold, De Rham cohomology theory teaches that the potential representations will be available only up to contributions from cohomology spaces of a small and finite dimension. They will not matter much for the overall performance of a preconditioner, and so we decided to forgo a discussion of general topologies.

The starting point for the development of the auxiliary space preconditioners presented in this paper is theoretical results that, roughly speaking, state that the gap between $(H^1(\Omega))^3$ and $\mathcal{H}(\mathbf{D}, \Omega)$ can be bridged by contributions from the kernel of \mathbf{D} . A rigorous statement is made by the following so-called regular decomposition

results. In light of the unified treatment we aim for, operators with similar function will be denoted alike, though they are different in **curl**- and **div**-contexts, respectively.

LEMMA 3.2 (existence of regular vector potentials [21, Lemma 2.5]). *There is a continuous mapping $\mathbf{L} : \{\mathbf{v} \in \mathbf{H}(\text{div}, \mathbb{R}^3), \text{div } \mathbf{v} = 0\} \mapsto (H^1(\mathbb{R}^3))^3$ such that $\mathbf{curl } \mathbf{L} \mathbf{v} = \mathbf{v}$ and $\text{div } \mathbf{L} \mathbf{v} = 0$.*

LEMMA 3.3 (regular decomposition of $\mathbf{H}(\mathbf{curl}, \Omega)$ [21, Lemma 2.4]). *There are continuous maps $\mathbf{R} : \mathbf{H}(\mathbf{curl}, \Omega) \mapsto (H^1(\Omega))^3$, $\mathbf{Z} : \mathbf{H}(\mathbf{curl}, \Omega) \mapsto H^1(\Omega)$ such that $\mathbf{R} + \mathbf{grad} \circ \mathbf{Z} = \text{Id}$ on $\mathbf{H}(\mathbf{curl}, \Omega)$ and $\mathbf{R} \mathbf{u} = 0 \Leftrightarrow \mathbf{curl } \mathbf{u} = 0$.*

LEMMA 3.4 (regular decomposition of $\mathbf{H}_0(\mathbf{curl}, \Omega)$ [32, section 2]). *There are continuous linear operators $\mathbf{R} : \mathbf{H}_0(\mathbf{curl}, \Omega) \mapsto (H_0^1(\Omega))^3$, $\mathbf{Z} : \mathbf{H}_0(\mathbf{curl}, \Omega) \mapsto H_0^1(\Omega)$ such that $\mathbf{R} + \mathbf{grad} \circ \mathbf{Z} = \text{Id}$ on $\mathbf{H}_0(\mathbf{curl}, \Omega)$ and $\mathbf{R} \mathbf{u} = 0 \Leftrightarrow \mathbf{curl } \mathbf{u} = 0$.*

COROLLARY 3.5. *Both operators \mathbf{R} introduced in Lemmas 3.3 and 3.4 satisfy*

$$\exists C = C(\Omega) > 0 : \quad \|\mathbf{R} \mathbf{v}\|_{H^1(\Omega)} \leq C \|\mathbf{curl } \mathbf{v}\|_{L^2(\Omega)} \quad \forall \mathbf{v} \in \mathcal{H}(\mathbf{curl}).$$

LEMMA 3.6 (existence of regular velocity fields, [17, Corollary 2.4]). *There is a continuous linear operator $\mathbf{K} : L_0^2(\Omega) := \{\mathbf{v} \in L^2(\Omega), \int_{\Omega} \mathbf{v} \, d\mathbf{x} = 0\} \mapsto (H_0^1(\Omega))^3$ such that $\text{div} \circ \mathbf{K} = \text{Id}$ on $L_0^2(\Omega)$.*

LEMMA 3.7 (regular decomposition of $\mathbf{H}(\text{div}, \Omega)$). *There are continuous linear operators $\mathbf{R} : \mathbf{H}(\text{div}, \Omega) \mapsto (H^1(\Omega))^3$, $\mathbf{Z} : \mathbf{H}(\text{div}, \Omega) \mapsto (H^1(\Omega))^3$ such that $\mathbf{R} + \mathbf{curl} \circ \mathbf{Z} = \text{Id}$ on $\mathbf{H}(\text{div}, \Omega)$ and $\mathbf{R} \mathbf{u} = 0 \Leftrightarrow \text{div } \mathbf{u} = 0$.*

Proof. For $\mathbf{u} \in \mathbf{H}(\text{div}, \Omega)$ perform a trivial extension by zero of $\text{div } \mathbf{u}$ to an element of $L^2(\mathbb{R}^3)$. By elementary Fourier transform techniques (see [17, section 3.3]) we establish the existence of $\mathbf{w} \in \mathbf{H}(\text{div}, \mathbb{R}^3)$ such that $\text{div } \mathbf{w} = \text{div } \mathbf{u}$ on Ω . Lemma 3.1 finishes the proof. \square

LEMMA 3.8 (regular decomposition of $\mathbf{H}_0(\text{div}, \Omega)$). *There are continuous linear operators $\mathbf{R} : \mathbf{H}_0(\text{div}, \Omega) \mapsto (H_0^1(\Omega))^3$, $\mathbf{Z} : \mathbf{H}_0(\text{div}, \Omega) \mapsto (H_0^1(\Omega))^3$ such that $\mathbf{R} + \mathbf{curl} \circ \mathbf{Z} = \text{Id}$ on $\mathbf{H}_0(\text{div}, \Omega)$ and $\mathbf{R} \mathbf{u} = 0 \Leftrightarrow \text{div } \mathbf{u} = 0$.*

Proof. Observe that $\text{div } \mathbf{H}_0(\text{div}, \Omega) \subset L_0^2(\Omega)$ and use Lemmas 3.6 and 3.1. \square

COROLLARY 3.9. *Both operators \mathbf{R} introduced in Lemmas 3.7 and 3.8 satisfy*

$$\exists C = C(\Omega) > 0 : \quad \|\mathbf{R} \mathbf{v}\|_{H^1(\Omega)} \leq C \|\text{div } \mathbf{v}\|_{L^2(\Omega)} \quad \forall \mathbf{v} \in \mathcal{H}(\text{div}).$$

Using the operator symbols from Table 3.1, we can summarize the above assertions in the following lemma.

LEMMA 3.10 (stable regular decomposition).

$$\begin{aligned} \exists \mathbf{R} \in L(\mathcal{H}(\mathbf{D}, \Omega), \mathcal{H}^1), \\ \exists \mathbf{Z} \in L(\mathcal{H}(\mathbf{D}, \Omega), \mathcal{H}(\mathbf{D}^-, \Omega)), : \quad \left\{ \begin{array}{l} \mathbf{R} + \mathbf{D}^- \circ \mathbf{Z} = \text{Id} \quad \text{on } \mathcal{H}(\mathbf{D}, \Omega), \\ \|\mathbf{R} \mathbf{v}\|_{H^1(\Omega)} \leq C \|\mathbf{D} \mathbf{v}\|_{L^2(\Omega)} \quad \forall \mathbf{v} \in \mathcal{H}(\mathbf{D}, \Omega), \\ \|\mathbf{Z} \mathbf{v}\|_{\mathcal{H}(\mathbf{D}^-, \Omega)} \leq C \|\mathbf{v}\|_{\mathcal{H}(\mathbf{D}, \Omega)} \quad \forall \mathbf{v} \in \mathcal{H}(\mathbf{D}, \Omega). \end{array} \right. \\ \exists C = C(\Omega) > 0 \end{aligned}$$

Proof. The assertion about \mathbf{R} rephrases those of Corollaries 3.5 and 3.9. Then

$$\begin{aligned} \|\mathbf{D}^- \mathbf{Z} \mathbf{v}\|_{L^2(\Omega)} &\leq \|\mathbf{R} \mathbf{v}\|_{L^2(\Omega)} + \|\mathbf{v}\|_{L^2(\Omega)} \\ &\leq C \|\mathbf{R} \mathbf{v}\|_{H^1(\Omega)} + \|\mathbf{v}\|_{L^2(\Omega)} \leq C \|\mathbf{D} \mathbf{v}\|_{L^2(\Omega)} + \|\mathbf{v}\|_{L^2(\Omega)}, \end{aligned}$$

and the estimate for the norm $\|\cdot\|_{\mathcal{H}(\mathbf{D}^-, \Omega)}$ can be inferred from the fact that $\mathbf{D}^- : \mathcal{H}(\mathbf{D}^-, \Omega) \mapsto L^2(\Omega)$ has closed range. \square

In light of the fictitious space lemma Theorem 2.2, the result of Lemma 3.10 can be read as follows (we refer the reader to Table 3.1 for the meaning of \mathcal{H}^1 and write

$(Id - \Delta) : \mathcal{H}^1 \mapsto (\mathcal{H}^1)'$ for the (second order elliptic) operator associated with the inner product of \mathcal{H}^1): the regular decomposition confirms that

$$(3.2) \quad B := I \circ (Id - \Delta)^{-1} \circ I^* + D^- \circ (Id + (D^-)^* D^-)^{-1} \circ (D^-)^*$$

will supply a “preconditioner” for the operator $A : \mathcal{H}(D, \Omega) \mapsto \mathcal{H}(D, \Omega)'$ induced by the bilinear form of (1.3). Here, I designates the trivial injection $I : \mathcal{H}^1 \mapsto \mathcal{H}(D, \Omega)$ arising from the continuous embedding $\mathcal{H}^1 \subset \mathcal{H}(D, \Omega)$. Applying Theorem 2.2 and (2.6) and recalling that $\|\Psi\|_{\mathcal{H}(D, \Omega)} \leq \|\Psi\|_{H^1(\Omega)}$, $\Psi \in \mathcal{H}(D^-, \Omega)$, and $\|D^- \varphi\|_{\mathcal{H}(D, \Omega)} \leq \|\varphi\|_{\mathcal{H}(D^-, \Omega)}$, $\varphi \in \mathcal{H}(D^-, \Omega)$, we readily conclude for $\tau = 1$

$$(3.3) \quad \kappa(BA) \leq \|R\|^2 + \|Z\|^2.$$

Of course, “preconditioning” an operator equation set in infinite-dimensional function spaces is hardly relevant for practical computations. Hence, the main objective of this paper is to get a discrete version of the above result.

Remark 3. All the above regular decompositions are global in the sense that the estimates of Corollaries 3.9 and 3.5 do not hold on subsets of Ω .

Remark 4. The regular decompositions outlined above have been widely used in functional analysis and numerical analysis connected with $\mathcal{H}(D, \Omega)$. In the study of function spaces and traces, some of them first appeared in [6] and were later used in [12, 15]. They have found their way into the theoretical analysis of multilevel methods [22, 26], domain decomposition methods [32], and boundary element methods [23].

A major shortcoming of the regular decompositions summarized in Lemma 3.10 is their lack of $L^2(\Omega)$ -stability. This is obviously guaranteed in the case of the classical $L^2(\Omega)$ -orthogonal Helmholtz decomposition

$$(3.4) \quad \mathcal{H}(D, \Omega) = \mathcal{H}(D0, \Omega) \oplus \mathcal{H}(D0, \Omega)^\perp.$$

However, the $L^2(\Omega)$ -orthogonal complement generally fails to belong to $H^1(\Omega)$ or $(H^1(\Omega))^3$, respectively. According to [17, section 3.4] this can only be taken for granted if $-\Delta$ with suitable homogeneous Dirichlet or Neumann boundary conditions is 2-regular on Ω (see [1] for details). We will refer to this situation as *the 2-regular case*. Conversely, Table 3.1 gives the meaning of the symbols in the *generic case*.

Remark 5. Convexity of Ω will ensure the 2-regular case. Moreover, for a convex Ω , formulas (2.8) and (2.3) in [16] involve the estimate

$$(3.5) \quad |R\mathbf{v}|_{H^1(\Omega)} \leq \|D\mathbf{v}\|_{L^2(\Omega)},$$

where $|\cdot|_{H^1(\Omega)}$ designates the componentwise $H^1(\Omega)$ -seminorm of a vector field.

However, use of the Helmholtz decomposition (3.4) entails relaxing the boundary conditions in $\mathcal{H}(D^-, \Omega)$, when boundary conditions are imposed on $\mathcal{H}(D, \Omega)$. More precisely, in the 2-regular case the following slightly modified meanings of the notation from Table 3.1 will be assumed. They are given in Table 3.2, where

$$\mathbf{H}_t^1(\Omega) := (H^1(\Omega))^3 \cap \mathbf{H}_0(\mathbf{curl}, \Omega), \quad \mathbf{H}_n^1(\Omega) := (H^1(\Omega))^3 \cap \mathbf{H}_0(\mathbf{div}, \Omega).$$

With (3.4) in mind, in the 2-regular case, the operators Z and R from Lemma (3.10) can be chosen to satisfy

$$(3.6) \quad \|D^- Z\mathbf{v}\|_{L^2(\Omega)}^2 + \|R\mathbf{v}\|_{L^2(\Omega)}^2 = \|\mathbf{v}\|_{L^2(\Omega)}^2 \quad \forall \mathbf{v} \in \mathcal{H}(D, \Omega).$$

TABLE 3.2
Symbols with altered meaning in the 2-regular case.

D	$\mathcal{H}(\mathbf{D}, \Omega)$	\mathbf{D}^-	$\mathcal{H}(\mathbf{D}^-, \Omega)$	\mathbf{D}^+	\mathcal{H}^1
curl	$\mathbf{H}_0(\mathbf{curl}, \Omega)$	grad	$H_0^1(\Omega)$	div	$\mathbf{H}_t^1(\Omega)$
div	$\mathbf{H}_0(\text{div}, \Omega)$	curl	$\mathbf{H}_0(\mathbf{curl}, \Omega)$	0	$\mathbf{H}_n^1(\Omega)$

In particular, \mathbf{Z} and $\mathbf{D}^- \circ \mathbf{Z}$ turn out to be the $L^2(\Omega)$ -orthogonal projections parallel to $\mathcal{H}(\mathbf{D}0, \Omega)$ and onto $\mathcal{H}(\mathbf{D}0, \Omega)$, respectively. The estimates of Corollaries 3.9 and 3.5 remain valid [1, section 2]. Thus, in the 2-regular case, Lemma 3.10 still holds with operators \mathbf{Z} and \mathbf{R} satisfying (3.6).

Remark 6. If Ω is a *polyhedron* (i.e., has flat faces), then we learn from Theorem 2.3 in [16] that

$$(3.7) \quad \|\mathbf{curl} \mathbf{u}\|_{L^2(\Omega)}^2 + \|\text{div} \mathbf{u}\|_{L^2(\Omega)}^2 = \|\mathbf{grad} \mathbf{u}\|_{L^2(\Omega)}^2 \quad \forall \mathbf{u} \in \mathbf{H}_t^1(\Omega) \cup \mathbf{H}_n^1(\Omega).$$

Whenever the definition of \mathbf{R} is based on the Helmholtz decomposition it will map into either $\mathbf{H}_t^1(\Omega)$ or $\mathbf{H}_n^1(\Omega)$ in the 2-regular case. Thus, we conclude that on a polyhedron in the 2-regular case

$$(3.8) \quad \|\mathbf{R}\mathbf{v}\|_{H^1(\Omega)} \leq \|\mathbf{v}\|_{\mathcal{H}(\mathbf{D}, \Omega)} \quad \forall \mathbf{v} \in \mathcal{H}(\mathbf{D}, \Omega) \quad \Rightarrow \quad \|\mathbf{R}\| = 1.$$

4. Finite element spaces. Essentially, the analysis of this paper applies to all the finite element subspaces of $\mathbf{H}(\mathbf{curl}, \Omega)$ and $\mathbf{H}(\text{div}, \Omega)$ that can be viewed as discrete differential forms. This includes the so-called first and second families of edge elements [29, 30] and Raviart–Thomas elements and the Brezzi–Douglas–Marini (BDM) elements [11, Chapter 4]. To keep the presentation focused, we discuss only the lowest order cases.

Examples for the lowest order $\mathcal{H}(\mathbf{D}, \Omega)$ -conforming finite element spaces on a tetrahedral mesh \mathcal{T}_h of Ω are listed in Table 4.1. They can be defined by

$$\begin{aligned} V_h(\mathbf{grad}) &:= \left\{ v_h \in \frac{H^1(\Omega)}{H_0^1(\Omega)} : v_h|_K(\mathbf{x}) = a + \mathbf{b} \cdot \mathbf{x}, a \in \mathbb{R}, \mathbf{b} \in \mathbb{R}^3, \forall K \in \mathcal{T}_h \right\}, \\ V_h(\mathbf{curl}) &:= \left\{ \mathbf{v}_h \in \frac{\mathbf{H}(\mathbf{curl}, \Omega)}{\mathbf{H}_0(\mathbf{curl}, \Omega)} : \mathbf{v}_h|_K(\mathbf{x}) = \mathbf{a} + \mathbf{x} \times \mathbf{b}, \mathbf{a}, \mathbf{b} \in \mathbb{R}^3, \forall K \in \mathcal{T}_h \right\}, \\ V_h(\text{div}) &:= \left\{ \mathbf{v}_h \in \frac{\mathbf{H}(\text{div}, \Omega)}{\mathbf{H}_0(\text{div}, \Omega)} : \mathbf{v}_h|_K(\mathbf{x}) = \mathbf{a} + \beta \mathbf{x}, \mathbf{a} \in \mathbb{R}^3, \beta \in \mathbb{R}, \forall K \in \mathcal{T}_h \right\}, \\ V_h(0) &:= \left\{ v_h \in \frac{L^2(\Omega)}{L_0^2(\Omega)} : v_h|_K(\mathbf{x}) = a, a \in \mathbb{R}, \forall K \in \mathcal{T}_h \right\}. \end{aligned}$$

For a thorough discussion the reader is referred to [21, Chapter 3] and [29]. Resorting to a unified notation, we use the symbol $V_h(\mathbf{D})$ for these spaces. Its concrete meaning in different contexts is specified in Table 4.1.

A fundamental property of these families of finite element spaces is that they permit a discrete counterpart of (3.1):

$$(4.1) \quad \text{Assumption 3.1} \quad \Rightarrow \quad V_h(\mathbf{D}0) := \{\mathbf{v}_h \in V_h(\mathbf{D}) : \mathbf{D}\mathbf{v}_h = 0\} = \mathbf{D}^- V_h(\mathbf{D}^-).$$

TABLE 4.1
Finite element spaces of Whitney forms.

D	$\mathcal{H}(\mathbf{D}, \Omega)$	$V_h(\mathbf{D}) \subset \mathcal{H}(\mathbf{D}, \Omega)$	FE space	Reference
grad	$H^1(\Omega)$ $H_0^1(\Omega)$	$V_h(\mathbf{grad})$	linear Lagrangian FE	[13]
curl	$\mathbf{H}(\mathbf{curl}, \Omega)$ $\mathbf{H}_0(\mathbf{curl}, \Omega)$	$V_h(\mathbf{curl})$	edge elements	[29]
div	$\mathbf{H}(\mathbf{div}, \Omega)$ $\mathbf{H}_0(\mathbf{div}, \Omega)$	$V_h(\mathbf{div})$	face elements	[29]
0	$L^2(\Omega)$ $L_0^2(\Omega)$	$V_h(0)$	p.w. constants	

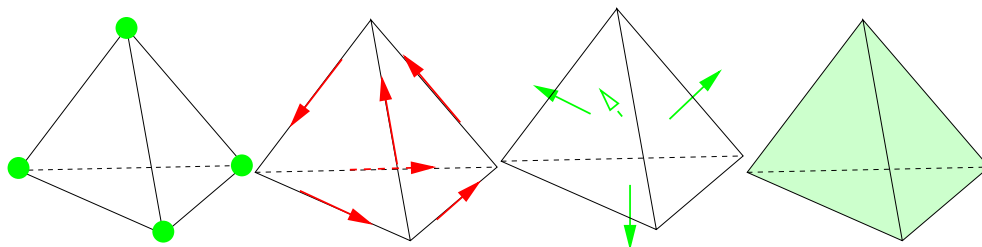


FIG. 4.1. Symbolic notation for local degrees of freedom for $V_h(\mathbf{grad})$, $V_h(\mathbf{curl})$, $V_h(\mathbf{div})$, and $V_h(0)$ (left to right).

These discrete potentials can even be chosen in a stable manner: with constants depending only on Ω , \mathbf{D} , and the shape regularity of \mathcal{T}_h ,

$$(4.2) \quad \forall \mathbf{v}_h \in V_h(\mathbf{D}0) : \quad \exists p_h \in V_h(\mathbf{D}^-) : \quad \mathbf{v}_h = \mathbf{D}^- p_h \quad \text{and} \quad \|p_h\|_{L^2(\Omega)} \lesssim \|\mathbf{v}_h\|_{L^2(\Omega)}.$$

For face elements this is a consequence of discrete Poincaré-type inequalities for $V_h(\mathbf{curl})$; see [21, Theorem 4.7]. For $\mathbf{D} = \mathbf{curl}$ and $\mathbf{D}^- = \mathbf{grad}$, (4.2) is just standard Poincaré–Friedrichs inequalities in $H^1(\Omega)/\mathbb{R}$ and $H_0^1(\Omega)$, respectively.

All the finite element spaces $V_h(\mathbf{D})$ are equipped with bases $\mathcal{B}(\mathbf{D})$ comprising locally supported functions; see [21, section 3.2]. These bases are L^2 -stable in the sense that

$$(4.3) \quad \mathbf{v}_h = \sum_{\mathbf{b} \in \mathcal{B}(\mathbf{D})} \mathbf{v}_{\mathbf{b}}, \quad \mathbf{v}_{\mathbf{b}} \in \text{span}\{\mathbf{b}\}, \quad \sum_{\mathbf{b} \in \mathcal{B}(\mathbf{D})} \|\mathbf{v}_{\mathbf{b}}\|_{L^2(\Omega)}^2 \approx \|\mathbf{v}_h\|_{L^2(\Omega)}^2 \quad \forall \mathbf{v}_h \in V_h(\mathbf{D}),$$

with constants¹ depending only on the shape regularity of \mathcal{T}_h ; see [24, section 2].

The spaces $V_h(\mathbf{D})$ also feature idempotent *nodal interpolation operators* $\Pi_h^{\mathbf{D}}$ whose range is $V_h(\mathbf{D})$. In the case $\mathbf{D} = \mathbf{grad}$ this is plain linear interpolation. For $\mathbf{D} = \mathbf{curl}$

¹By the symbols \approx , \lesssim , and \gtrsim we designate two- or one-sided inequalities, respectively, that hold up to multiplication of one side with a positive constant. In inequalities involving norms on function spaces this constant must not depend on the choice of functions. It may not depend on other problem and discretization parameters, and this will always be made clear.

the interpolation is based on path integrals along edges

$$(4.4) \quad \Pi_h^{\text{curl}} \mathbf{v} = \sum_{e \in \mathcal{E}_h} \int_e \mathbf{v} \cdot d\vec{s} \cdot \mathbf{b}_e,$$

where \mathcal{E}_h is the set of (interior) edges of \mathcal{T}_h and \mathbf{b}_e is the edge element basis function associated with the edge e . For $\mathbf{D} = \text{div}$, the interpolation relies on face fluxes:

$$(4.5) \quad \Pi_h^{\text{div}} \mathbf{v} = \sum_{f \in \mathcal{F}_h} \int_f \mathbf{v} \cdot d\mathbf{S} \cdot \mathbf{b}_f,$$

with \mathcal{F}_h designating the set of (interior) faces of \mathcal{T}_h . The relevant domains of integration for interpolation are depicted in Figure 4.1. Finally, the “interpolation” onto $V_h(0)$ agrees with $L^2(\Omega)$ -projection. All these operators are well defined for continuous functions/vector fields, unbounded on $\mathcal{H}(\mathbf{D}, \Omega)$ (except for $V_h(0)$), and possess the exceptional *commuting diagram property*

$$(4.6) \quad \mathbf{D} \circ \Pi_h^{\mathbf{D}} = \Pi_h^+ \circ \mathbf{D} \quad \text{on domain of } \Pi_h^{\mathbf{D}}, \quad \Pi_h^+ := \Pi_h^{\mathbf{D}^+}.$$

A concise way of writing (4.1) and (4.6) is through combined exact sequences and commuting diagrams:

$$\begin{array}{ccccccccc} 0 & \longrightarrow & C^\infty(\Omega) & \xrightarrow{\text{grad}} & (C^\infty(\Omega))^3 & \xrightarrow{\text{curl}} & (C^\infty(\Omega))^3 & \xrightarrow{\text{div}} & C^\infty(\Omega) & \longrightarrow & 0 \\ & & \downarrow \Pi_h^{\text{grad}} & & \downarrow \Pi_h^{\text{curl}} & & \downarrow \Pi_h^{\text{div}} & & \downarrow \Pi_h^0 & & \\ 0 & \longrightarrow & V_h(\text{grad}) & \xrightarrow{\text{grad}} & V_h(\text{curl}) & \xrightarrow{\text{curl}} & V_h(\text{div}) & \xrightarrow{\text{div}} & V_h(0) & \longrightarrow & 0. \end{array}$$

We write $h \in L^\infty(\Omega)$ for the piecewise constant meshwidth function, which assumes value $h|_K := \text{diam}(K)$ in each cell K of \mathcal{T}_h . Using this function, we can state the following interpolation error estimate (see [21, section 3.6] and [21, Lemma 4.6]).

LEMMA 4.1. *The interpolation operators $\Pi_h^{\mathbf{D}}$ are bounded on $\{\mathbf{v} \in \mathcal{H}^1, \mathbf{D}\mathbf{v} \in V_h(\mathbf{D}^+)\} \subset \mathcal{H}^1$ and, with constants merely depending on \mathbf{D} and the shape regularity of \mathcal{T}_h , they satisfy*

$$(4.7) \quad \|h^{-1}(\text{Id} - \Pi_h^{\mathbf{D}})\Psi\|_{L^2(\Omega)} \lesssim \|\Psi\|_{H^1(\Omega)} \quad \forall \Psi \in \mathcal{H}^1, \mathbf{D}\mathbf{v} \in V_h(\mathbf{D}^+).$$

Simple affine equivalence techniques also yield the inverse estimate

$$(4.8) \quad \|\mathbf{D}\mathbf{v}_h\|_{L^2(\Omega)} \lesssim \|h^{-1}\mathbf{v}_h\|_{L^2(\Omega)} \quad \forall \mathbf{v} \in V_h(\mathbf{D}),$$

with a constant depending only on \mathbf{D} and the shape regularity of the mesh.

The role of the discrete auxiliary space will be played by the finite element space $S_h \subset \mathcal{H}^1$ of continuous functions or vector fields, whose Cartesian components are piecewise linear. We point out that

$$(4.9) \quad \mathbf{D}S_h \subset \mathbf{D}V_h(\mathbf{D}), \quad \mathbf{D} \in \{\text{grad}, \text{curl}, \text{div}\}.$$

Thanks to the commuting diagram property, we immediately conclude

$$(4.10) \quad \mathbf{D}\Pi_h^{\mathbf{D}}\Psi_h = \Pi_h^+\mathbf{D}\Psi_h = \mathbf{D}\Psi_h \quad \forall \Psi_h \in S_h.$$

Moreover, straightforward scaling arguments bear out that, with constants depending only on the shape regularity of \mathcal{T}_h ,

$$(4.11) \quad \|\mathbf{D}\Pi_h^{\mathbf{D}}\Psi_h\|_{L^2(\Omega)} \lesssim \|\Psi_h\|_{H^1(\Omega)}, \quad \|\Pi_h^{\mathbf{D}}\Psi_h\|_{L^2(\Omega)} \lesssim \|\Psi_h\|_{L^2(\Omega)} \quad \forall \Psi_h \in S_h.$$

Finally, we recall the surjective and idempotent quasi-interpolation operators for Lagrangian finite element spaces introduced in [34]. We may apply them to the components of vector fields separately. In the generic case (see Table 3.1), this gives rise to the projectors $\tilde{\mathbf{Q}}_h : \mathcal{H}^1 \mapsto S_h$, which inherit the continuity

$$(4.12) \quad \|\tilde{\mathbf{Q}}_h\Psi\|_{H^1(\Omega)} \lesssim \|\Psi\|_{H^1(\Omega)} \quad \forall \Psi \in \mathcal{H}^1,$$

respect possible boundary values in the sense that $\tilde{\mathbf{Q}}_h(H_0^1(\Omega))^3 \subset (H_0^1(\Omega))^3$, and satisfy the local projection error estimate

$$(4.13) \quad \|h^{-1}(\tilde{\mathbf{Q}}_h - Id)\Psi\|_{L^2(\Omega)} \lesssim \|\Psi\|_{H^1(\Omega)} \quad \forall \Psi \in \mathcal{H}^1.$$

In the 2-regular case (see the end of section 3 for a discussion and Table 3.2 for the slightly changed meanings of symbols), we will replace $\tilde{\mathbf{Q}}_h$ with the $L^2(\Omega)$ -orthogonal projections $\mathbf{Q}_h : (L^2(\Omega))^3 \mapsto S_h$. From interpolation arguments we readily infer the estimate

$$(4.14) \quad \|h^{-1}(\mathbf{Q}_h - Id)\Psi\|_{L^2(\Omega)} \lesssim \|\Psi\|_{H^1(\Omega)} \quad \forall \Psi \in \mathcal{H}^1,$$

but this time, in contrast to (4.13), the constants will *also* depend on the quasi-uniformity of the mesh. So, h in (4.14) should be read as the global meshwidth of \mathcal{T}_h . The approximation property also involves the continuity

$$(4.15) \quad \|\mathbf{Q}_h\Psi\|_{H^1(\Omega)} \lesssim \|\Psi\|_{H^1(\Omega)} \quad \forall \Psi \in \mathcal{H}^1,$$

again, with quasi-uniformity of the mesh also entering the constants.

Summing up, whenever we can take quasi-uniformity of the meshes for granted, \mathbf{Q}_h can replace $\tilde{\mathbf{Q}}_h$ with the extra benefit of $L^2(\Omega)$ -continuity.

5. Discrete regular decompositions. Now, following [25], let us derive a discrete version of the above regular decomposition results of section 3. First, we focus on the generic case; see Table 3.1. We fix a $\mathbf{v}_h \in V_h(\mathbf{D})$ and use the stable regular decomposition of Lemma 3.10 to split it according to

$$(5.1) \quad \mathbf{v}_h = \Psi + \mathbf{D}^-p, \quad \Psi := \mathbf{R}\mathbf{v}_h \in \mathcal{H}^1, \quad p := \mathbf{Z}\mathbf{v}_h \in \mathcal{H}(\mathbf{D}^-, \Omega).$$

We already know that the functions Ψ and p satisfy

$$(5.2) \quad \|\Psi\|_{H^1(\Omega)} \lesssim \|\mathbf{D}\mathbf{v}_h\|_{L^2(\Omega)}, \quad \|\mathbf{D}^-p\|_{L^2(\Omega)} \lesssim \|\mathbf{v}_h\|_{\mathcal{H}(\mathbf{D}, \Omega)},$$

with constants depending only on Ω .

So far, (5.1) is useless in the context of practical fictitious space preconditioning, because both Ψ and p fail to be finite element functions. The challenge is to convert (5.1) into a purely discrete decomposition without squandering the stability expressed by (5.2). This can be achieved only by incorporating another “high-frequency” contribution. Eventually, that forces us to incorporate a smoothing procedure into the algorithm.

LEMMA 5.1. For any \mathbf{v}_h there is $\Psi_h \in S_h$, $p_h \in V_h(\mathcal{D}^-)$, and $\tilde{\mathbf{v}}_h \in V_h(\mathcal{D})$ such that

$$(5.3) \quad \mathbf{v}_h = \tilde{\mathbf{v}}_h + \Pi_h^{\mathcal{D}} \Psi_h + \mathcal{D}^- p_h,$$

and

$$(5.4) \quad \|h^{-1} \tilde{\mathbf{v}}_h\|_{L^2(\Omega)}^2 + \|\Psi_h\|_{H^1(\Omega)}^2 \lesssim \|\mathcal{D} \mathbf{v}_h\|_{L^2(\Omega)}^2, \quad \|p_h\|_{\mathcal{H}(\mathcal{D}^-, \Omega)} \lesssim \|\mathbf{v}_h\|_{\mathcal{H}(\mathcal{D}, \Omega)}.$$

The constants are allowed to depend on Ω and the shape regularity of the mesh.

Proof. First, note that in (5.1) $\mathcal{D} \Psi = \mathcal{D} \mathbf{v}_h \in V_h(\mathcal{D}^+)$, and, owing to Lemma 4.1, $\Pi_h^{\mathcal{D}} \Psi$ is well defined. Further, the commuting diagram property implies

$$(5.5) \quad \mathcal{D} \Pi_h^{\mathcal{D}} \Psi = \Pi_h^{\mathcal{D}} \mathcal{D} \Psi = \mathcal{D} \Psi \Rightarrow \mathcal{D} (Id - \Pi_h^{\mathcal{D}}) \Psi = 0.$$

This confirms that the third term in the splitting

$$(5.6) \quad \Psi = \Pi_h^{\mathcal{D}} (\Psi - \tilde{\mathcal{Q}}_h \Psi) + \Pi_h^{\mathcal{D}} \tilde{\mathcal{Q}}_h \Psi + (Id - \Pi_h^{\mathcal{D}}) \Psi$$

actually belongs to the kernel of \mathcal{D} . By (4.1), we conclude

$$(5.7) \quad \exists q \in \mathcal{H}(\mathcal{D}^-, \Omega) : (Id - \Pi_h^{\mathcal{D}}) \Psi = \mathcal{D}^- q,$$

and (4.7) together with (5.2) yields

$$(5.8) \quad \|h^{-1} \mathcal{D}^- q\|_{L^2(\Omega)} = \|h^{-1} (Id - \Pi_h^{\mathcal{D}}) \Psi\|_{L^2(\Omega)} \lesssim \|\Psi\|_{H^1(\Omega)} \lesssim \|\mathcal{D} \mathbf{v}_h\|_{L^2(\Omega)}.$$

Thus, we can define the terms in the decomposition (5.3) as

$$(5.9) \quad \tilde{\mathbf{v}}_h := \Pi_h^{\mathcal{D}} (\Psi - \tilde{\mathcal{Q}}_h \Psi) \in V_h(\mathcal{D}),$$

$$(5.10) \quad \Psi_h := \tilde{\mathcal{Q}}_h \Psi \in S_h,$$

$$(5.11) \quad \mathcal{D}^- p_h := \mathcal{D}^- (p + q), \quad p_h \in V_h(\mathcal{D}^-).$$

Indeed, $\mathcal{D}^- (p + q) \in V_h(\mathcal{D})$ such that we can add a contribution from $\mathcal{H}(\mathcal{D}^-, \Omega)$ to $p + q$ and obtain a discrete function. Thanks to (4.2) we can guarantee that $\|p_h\|_{L^2(\Omega)} \lesssim \|\mathcal{D}^- p_h\|_{L^2(\Omega)}$; this will not affect the decomposition. The stability of the decomposition (5.3) can be established as follows: first, make use of Lemma 4.1 and (4.13) to obtain

$$\begin{aligned} \|h^{-1} \tilde{\mathbf{v}}_h\|_{L^2(\Omega)} &\leq \|h^{-1} (Id - \Pi_h^{\mathcal{D}}) (\Psi - \tilde{\mathcal{Q}}_h \Psi)\|_{L^2(\Omega)} + \|h^{-1} (Id - \tilde{\mathcal{Q}}_h) \Psi\|_{L^2(\Omega)} \\ &\lesssim \|(Id - \tilde{\mathcal{Q}}_h) \Psi\|_{H^1(\Omega)} + \|\Psi\|_{H^1(\Omega)} \\ &\lesssim \|\Psi\|_{H^1(\Omega)} \lesssim \|\mathcal{D} \mathbf{v}_h\|_{L^2(\Omega)}. \end{aligned}$$

Due to the definition (5.10), the next estimate is a simple consequence of (4.12) and Lemma 3.10:

$$(5.12) \quad \|\Psi_h\|_{H^1(\Omega)} \lesssim \|\Psi\|_{H^1(\Omega)} \lesssim \|\mathcal{D} \mathbf{v}_h\|_{L^2(\Omega)}.$$

Finally, the estimates established so far plus the triangle inequality yield

$$(5.13) \quad \|\mathcal{D}^- p_h\|_{L^2(\Omega)} \lesssim \|\mathbf{v}_h\|_{L^2(\Omega)} + \|\mathcal{D} \mathbf{v}_h\|_{L^2(\Omega)}.$$

Owing to the discrete Poincaré–Friedrichs inequality (4.2), this implies (5.4). \square

Remark 7. It is worth noting (see Table 3.1) that homogeneous boundary conditions imposed on $\mathcal{H}(\mathbf{D}, \Omega)$ permit us to choose $S_h \subset (H_0^1(\Omega))^3$. This means that Ψ_h will completely vanish on $\partial\Omega$, though it is only the tangential or normal components of \mathbf{v}_h , respectively, that vanish on $\partial\Omega$.

LEMMA 5.2. *In the 2-regular case (see section 3, Table 3.2) the splitting (5.3) from Lemma 5.1 can be chosen such that, in addition to the estimates asserted in Lemma 5.1, we have*

$$\|\mathbf{D}^- p_h\|_{L^2(\Omega)} \lesssim \|\mathbf{v}_h\|_{L^2(\Omega)}, \quad \|\Psi_h\|_{L^2(\Omega)} \lesssim \|\mathbf{v}_h\|_{L^2(\Omega)},$$

with constants additionally depending on the quasi-uniformity of the mesh \mathcal{T}_h .

Proof. We rely on the $L^2(\Omega)$ -orthogonal Helmholtz decomposition (3.4) to define p and Ψ in (5.1). Consequently, we can expect

$$(5.14) \quad \|\Psi\|_{L^2(\Omega)} \leq \|\mathbf{v}_h\|_{L^2(\Omega)}, \quad \|\mathbf{D}^- p\|_{L^2(\Omega)} \leq \|\mathbf{v}_h\|_{L^2(\Omega)}.$$

Then follow the proof of Lemma 5.1 and replace the quasi-interpolation $\tilde{\mathbf{Q}}_h$ with the $L^2(\Omega)$ -orthogonal projection \mathbf{Q}_h . Taking into account that h designates a global meshwidth when the constants are allowed to depend on quasi-uniformity, a glance at (4.14) and (4.15) confirms that all estimates of Lemma 5.1 remain true.

The replacement of $\tilde{\mathbf{Q}}_h$ is necessary, because $\tilde{\mathbf{Q}}_h$ fails to be continuous with respect to the $L^2(\Omega)$ -norm. When using \mathbf{Q}_h instead, we arrive at the trivial estimate

$$(5.15) \quad \Psi_h := \mathbf{Q}_h \Psi \quad \Rightarrow \quad \|\Psi_h\|_{L^2(\Omega)} \leq \|\Psi\|_{L^2(\Omega)} \leq \|\mathbf{v}_h\|_{L^2(\Omega)}.$$

In addition, use the interpolation estimate (5.8) and the inverse inequality (4.8):

$$(5.16) \quad \|\mathbf{D}^- q\|_{L^2(\Omega)} \lesssim h \|\mathbf{D} \mathbf{v}_h\|_{L^2(\Omega)} \lesssim \|\mathbf{v}_h\|_{L^2(\Omega)}.$$

Again, h denotes the (global) meshwidth of \mathcal{T}_h . Owing to (5.11) and (5.14), this finishes the proof. \square

6. Stable splittings. We first discuss the case $0 < \tau \leq 1$; that is, the second order term in the bilinear form is dominant. The notation refers to the generic case of Table 3.1.

THEOREM 6.1. *Assume $0 < \tau \leq 1$. For any $\mathbf{v}_h \in V_h(\mathbf{D})$ there is $p_h \in V_h(\mathbf{D}^-)$, $\Psi_h \in S_h$ such that, when $\mathbf{v}_b \in \text{span}\{\mathbf{b}\}$, $\mathbf{b} \in \mathcal{B}(\mathbf{D})$, a locally supported basis function,*

$$(6.1) \quad \sum_{\mathbf{b} \in \mathcal{B}(\mathbf{D})} \mathbf{v}_b + \Pi_h^{\mathbf{D}} \Psi_h + \mathbf{D}^- p_h = \mathbf{v}_h,$$

$$(6.2) \quad \sum_{\mathbf{b} \in \mathcal{B}(\mathbf{D})} \|\mathbf{v}_b\|_A^2 + \|\Psi_h\|_{H^1(\Omega)}^2 + \|\mathbf{D}^- p_h\|_A^2 \lesssim \|\mathbf{v}_h\|_A^2,$$

with a constant depending only on Ω , \mathbf{D} , and the shape regularity of \mathcal{T}_h , but independent of $\tau \in]0, 1]$ and quasi-uniformity.

Proof. The contributions Ψ_h and p_h are chosen as in Lemma 5.1. Hence, reusing the notation of (5.3),

$$(6.3) \quad \sum_{\mathbf{b} \in \mathcal{B}(\mathbf{D})} \mathbf{v}_b = \tilde{\mathbf{v}}_h.$$

By the inverse estimate (4.8), (4.3), and the bound for $\|h^{-1}\tilde{\mathbf{v}}_h\|$ from Lemma 5.1

$$\begin{aligned}
 \sum_{\mathbf{b} \in \mathcal{B}(\mathbf{D})} \|\mathbf{v}_{\mathbf{b}}\|_A^2 &= \sum_{\mathbf{b} \in \mathcal{B}(\mathbf{D})} \|\mathbf{D}\mathbf{v}_{\mathbf{b}}\|_{L^2(\Omega)}^2 + \tau \|\mathbf{v}_{\mathbf{b}}\|_{L^2(\Omega)}^2 \\
 (6.4) \quad &\lesssim \sum_{\mathbf{b} \in \mathcal{B}(\mathbf{D})} \|h^{-1}\mathbf{v}_{\mathbf{b}}\|_{L^2(\Omega)}^2 + \tau \sum_{\mathbf{b} \in \mathcal{B}(\mathbf{D})} \|\mathbf{v}_{\mathbf{b}}\|_{L^2(\Omega)}^2 \\
 &\lesssim \|h^{-1}\tilde{\mathbf{v}}_h\|_{L^2(\Omega)}^2 + \tau \|\tilde{\mathbf{v}}_h\|_{L^2(\Omega)}^2 \lesssim \|\mathbf{D}\mathbf{v}_h\|_{L^2(\Omega)}^2 + \tau \|\mathbf{v}_h\|_{L^2(\Omega)}^2.
 \end{aligned}$$

The remaining bounds are immediate from Lemma 5.1 because

$$\|\mathbf{D}^-p_h\|_A^2 = \|\mathbf{D}\mathbf{D}^-p_h\|_{L^2(\Omega)}^2 + \tau \|\mathbf{D}^-p_h\|_{L^2(\Omega)}^2 = \tau \|\mathbf{D}^-p_h\|_{L^2(\Omega)}^2.$$

All the constants merely depend on Ω and the shape regularity of \mathcal{T}_h . \square

The case $\mathbf{D} = \text{div}$ deserves special attention, because the discrete potential belongs to $V_h(\mathbf{curl})$. This is not entirely desirable, because it entails solving an $\mathbf{H}(\mathbf{curl}, \Omega)$ -elliptic problem in $V_h(\mathbf{curl})$ when evaluating the preconditioner. Yet, as $\mathbf{curl} \circ \mathbf{grad} = 0$, we can apply the decomposition of Theorem 6.1 recursively and replace $p_h \in V_h(\mathbf{curl})$ by a $\Phi_h \in S_h$ and some “high-frequency” edge element function.

Thus, for $\mathbf{D} = \text{div}$ and $\mathbf{v}_h \in V_h(\text{div})$, we examine the decomposition

$$\begin{aligned}
 \mathbf{v}_h &= \sum_{\mathbf{b} \in \mathcal{B}(\text{div})} \mathbf{v}_{\mathbf{b}} + \Pi_h^{\text{div}} \Psi_h + \mathbf{curl} p_h \\
 (6.5) \quad &= \sum_{\mathbf{b} \in \mathcal{B}(\text{div})} \mathbf{v}_{\mathbf{b}} + \Pi_h^{\text{div}} \Psi_h + \sum_{\mathbf{q} \in \mathcal{B}(\mathbf{curl})} \mathbf{curl} p_{\mathbf{q}} + \mathbf{curl} \Phi_h,
 \end{aligned}$$

where $\Psi_h, \Phi_h \in S_h$ and

$$\mathbf{v}_{\mathbf{b}} \in \text{span}\{\mathbf{b}\}, \quad \mathbf{b} \in \mathcal{B}(\text{div}), \quad p_{\mathbf{q}} \in \text{span}\{\mathbf{q}\}, \quad \mathbf{q} \in \mathcal{B}(\mathbf{curl}).$$

From Theorem 6.1 we conclude that for $0 < \tau \leq 1$

$$\sum_{\mathbf{b} \in \mathcal{B}(\text{div})} \|\mathbf{v}_{\mathbf{b}}\|_A^2 + \|\Psi_h\|_{H^1(\Omega)}^2 + \tau \sum_{\mathbf{q} \in \mathcal{B}(\mathbf{curl})} \|\mathbf{curl} p_{\mathbf{q}}\|_{L^2(\Omega)}^2 + \tau \|\Phi_h\|_{H^1(\Omega)}^2 \lesssim \|\mathbf{v}_h\|_A^2. \quad (6.6)$$

From now on we permit dependence of the constants on the variation of h . In other words, the estimates below hinge on the assumption of quasi-uniformity of the mesh \mathcal{T}_h , which permits us to assume a global meshwidth $h > 0$. Then, we can establish stability *uniformly* for all $\tau > 0$.

THEOREM 6.2. *Assume the 2-regular case. Then, for all $\mathbf{v}_h \in V_h(\mathbf{D})$, we can find $p_h \in V_h(\mathbf{D}^-)$, $\Psi_h \in S_h$ such that, when $\mathbf{v}_{\mathbf{b}} \in \text{span}\{\mathbf{b}\}$, $\mathbf{b} \in \mathcal{B}(\mathbf{D})$,*

$$\sum_{\mathbf{b} \in \mathcal{B}(\mathbf{D})} \mathbf{v}_{\mathbf{b}} + \Pi_h^{\mathbf{D}} \Psi_h + \mathbf{D}^-p_h = \mathbf{v}_h, \quad (6.7)$$

$$\sum_{\mathbf{b} \in \mathcal{B}(\mathbf{D})} \|\mathbf{v}_{\mathbf{b}}\|_A^2 + \|\Psi_h\|_{H^1(\Omega)}^2 + \tau \|\Psi_h\|_{L^2(\Omega)}^2 + \|\mathbf{D}^-p_h\|_A^2 \lesssim \|\mathbf{v}_h\|_A^2, \quad (6.8)$$

with a constant depending only on Ω , \mathbf{D} , and the shape regularity and quasi-uniformity of \mathcal{T}_h , but independent of $\tau \geq 0$.

Proof. We rely on the decomposition established in Lemma 5.2,

$$(6.9) \quad \mathbf{v}_h = \tilde{\mathbf{v}}_h + \Pi_h^D \Psi_h + D^- p_h,$$

and find, using (4.8), (6.3), and (3.6),

$$(6.10) \quad \begin{aligned} \sum_{\mathbf{b} \in \mathcal{B}(D)} \|\mathbf{v}_b\|_A^2 &\lesssim \sum_{\mathbf{b} \in \mathcal{B}(D)} h^{-2} \|\mathbf{v}_b\|_{L^2(\Omega)}^2 + \tau \sum_{\mathbf{b} \in \mathcal{B}(D)} \|\mathbf{v}_b\|_{L^2(\Omega)}^2 \\ &\lesssim (h^{-2} + \tau) \|\tilde{\mathbf{v}}_h\|_{L^2(\Omega)}^2 \lesssim (h^{-2} + \tau) h^2 \|D \mathbf{v}_h\|_{L^2(\Omega)}^2 \\ &\lesssim \|D \mathbf{v}_h\|_{L^2(\Omega)}^2 + \tau \|\mathbf{v}_h\|_{L^2(\Omega)}^2. \end{aligned}$$

Bounds for the other terms are straightforward from the estimates of Lemmas 5.2 and 5.1. \square

As regards $D = \text{div}$, in the 2-regular case we also get a τ -uniform estimate for the splitting (6.5):

$$(6.11) \quad \begin{aligned} \sum_{\mathbf{b} \in \mathcal{B}(\text{div})} \|\mathbf{v}_b\|_A^2 + \|\Psi_h\|_{H^1(\Omega)}^2 + \tau \|\Psi_h\|_{L^2(\Omega)}^2 \\ + \tau \sum_{\mathbf{b} \in \mathcal{B}(\text{curl})} \|\text{curl } p_b\|_{L^2(\Omega)}^2 + \tau \|\Phi_h\|_{H^1(\Omega)}^2 \lesssim \|\mathbf{v}_h\|_A^2. \end{aligned}$$

Remark 8. The theory seems to indicate increased robustness of the preconditioner with respect to $\tau \rightarrow \infty$ in the 2-regular case. However, the numerical experiments of section 8 send the unequivocal message that the “generic case” version of the preconditioner does not deteriorate as τ becomes large. Here, theory obviously falls short of capturing the actual behavior of the method.

7. Auxiliary space preconditioners. We start from the stable decompositions of $V_h(D)$ introduced in Theorems 6.1 and 6.2 and (6.5) and apply the abstract theory of section 2 for $V = V_h(D)$ and the energy bilinear form $a(\cdot, \cdot)$ from (1.3).

Throughout, let \mathbf{A}_D denote the Galerkin matrix arising from (1.3) with respect to the standard basis $\mathcal{B}(D)$ of $V_h(D)$. We write \mathbf{L} for the matrix related to the bilinear form

$$(\Psi, \Phi) \mapsto (\text{grad } \Psi, \text{grad } \Phi)_0, \quad \Phi, \Psi \in \mathcal{H}^1,$$

on S_h , which is endowed with the usual nodal basis of hat functions (for the components of vector fields). The positive definite mass matrix on S_h , that is, the Galerkin matrix for the $L^2(\Omega)$ -inner product, will be designated by \mathbf{M} . Further, we adopt the notation \mathbf{P}_D for the matrix describing the mapping $\Pi_h^D : \mathcal{H}^1 \mapsto V_h(D)$ with respect to the “hat function basis” of \mathcal{H}^1 and the basis $\mathcal{B}(D)$ of $V_h(D)$.

We restrict ourselves to Jacobi smoothing; that is, the smoothing operator is characterized by the inner product

$$(7.1) \quad s(\mathbf{v}_h, \mathbf{v}_h) = \sum_{\mathbf{b} \in \mathcal{B}(D)} a(\mathbf{v}_b, \mathbf{v}_b), \quad \sum_{\mathbf{b} \in \mathcal{B}(D)} \mathbf{v}_b = \mathbf{v}_h, \quad \mathbf{v}_b \in \text{span}\{\mathbf{b}\},$$

and its matrix representation coincides with the diagonal \mathbf{D}_A of \mathbf{A}_D . More generally, one could use any $s(\cdot, \cdot)$ that features the spectral equivalence $s(\mathbf{v}_h, \mathbf{v}_h) \approx \|h^{-1} \mathbf{v}_h\|_{L^2(\Omega)}^2 + \tau \|\mathbf{v}_h\|^2$.

Since the square of the energy norm can be computed by summing local contributions from the cells K of the mesh \mathcal{T}_h , we find

$$(7.2) \quad \begin{aligned} \|\mathbf{v}_h\|_A^2 &= \left\| \sum_{\mathbf{b} \in \mathcal{B}(\mathcal{D})} \alpha_{\mathbf{b}} \mathbf{b} \right\|_A^2 = \sum_{K \in \mathcal{T}_h} \left\| \sum_{j=1}^M \alpha_{K,j} \mathbf{b}_{K,j} \right\|_A^2 \\ &\leq M \sum_K \sum_{\mathbf{b} \in \mathcal{B}(\mathcal{D})} |\alpha_{\mathbf{b}}|^2 \|\mathbf{b}\|_A^2 = M \sum_{\mathbf{b} \in \mathcal{B}(\mathcal{D})} |\alpha_{\mathbf{b}}|^2 \|\mathbf{b}\|_A^2 = Ms(\mathbf{v}, \mathbf{v}) \end{aligned}$$

if $\mathbf{v}_h = \sum_{\mathbf{b} \in \mathcal{B}(\mathcal{D})} \alpha_{\mathbf{b}} \mathbf{b} \in V_h(\mathcal{D})$. Here, M bounds the (small) number of basis functions whose support overlaps with a single element K . This implies that c_s in (2.12) can be chosen as a small universal constant.

For the sake of simplicity, we continue the discussion for the cases $\mathcal{D} = \mathbf{curl}$ (edge elements) and $\mathcal{D} = \mathbf{div}$ (face elements) separately.

7.1. A preconditioner for $\mathbf{H}(\mathbf{curl}, \Omega)$ -elliptic problems. We rely on the splitting (6.1) to define the preconditioner. This means that, in terms of the concepts developed in section 2, we have two auxiliary spaces:

1. The space $W_1 := S_h$ with inner product $\bar{a}_1(\Psi_h, \Psi_h) := \|\Psi_h\|_{H^1(\Omega)}^2 + \tau \|\Psi_h\|_{L^2(\Omega)}^2$, which is suggested by (6.2) and (6.8). The corresponding transfer operator is $\Pi_1 := \Pi_h^{\mathbf{curl}}$, and, thanks to (4.11), (2.11) holds with constant c_1 depending only on the shape regularity of the mesh.
2. The discrete potential space $W_2 := V_h(\mathcal{D}^-)$ equipped with inner product $\bar{a}_2(p_h, p_h) := \tau |p_h|_{H^1(\Omega)}^2$ and transfer operator $\Pi_2 := \mathbf{grad} : V_h(\mathcal{D}^-) \mapsto V_h(\mathcal{D})$, whose norm is uniformly bounded by 1.

We write \mathbf{G} for the matrix related to $\mathbf{grad} : V_h(\mathcal{D}^-) \mapsto V_h(\mathcal{D})$ and Δ for the discrete Laplacian (matrix) on linear Lagrangian finite element space $V_h(\mathbf{grad})$. Then the matrix of the resulting auxiliary space preconditioner for the $\mathbf{H}(\mathbf{curl}, \Omega)$ -elliptic problem (1.1) reads

$$(7.3) \quad \mathbf{B}_{\mathbf{curl}} := \mathbf{D}_A^{-1} + \mathbf{P}_{\mathbf{curl}}(\mathbf{L} + \tau \mathbf{M})^{-1} \mathbf{P}_{\mathbf{curl}}^T + \tau^{-1} \mathbf{G}(-\Delta)^{-1} \mathbf{G}^T.$$

THEOREM 7.1. *For $0 < \tau \leq 1$ the spectral condition number $\kappa(\mathbf{B}_{\mathbf{curl}} \mathbf{A}_{\mathbf{curl}})$ depends only on Ω and the shape regularity of the mesh.*

In the 2-regular case $\kappa(\mathbf{B}_{\mathbf{curl}} \mathbf{A}_{\mathbf{curl}})$ is bounded independently of τ , but the quasi-uniformity of the mesh may affect the bound.

Proof. Theorems 6.1 and 6.2 provide the bound for c_0 from (2.13). The constants c_s and c_1, c_2 have been discussed before. Thus, (2.14) leads to the assertion of the theorem. \square

The impact of switching to spectrally equivalent bilinear forms on W_1, W_2 can be gauged as in Corollary 2.3.

We point out that the transfers can be realized by purely local operations; see [5, section 3] and [5, section 5]. In detail, assuming the standard bases, gradient-matrix \mathbf{G} will agree with the edge-vertex incidence matrix of the mesh. The matrix $\mathbf{P}_{\mathbf{curl}}$ connected with the interpolation $\Pi_h^{\mathbf{curl}}$ describes a local distribution of vectorial degrees of freedom attached to the nodes of the mesh to adjacent edges: the edge connecting vertices with values \mathbf{w}_1 and \mathbf{w}_2 receives the value

$$(7.4) \quad \frac{1}{2}(\mathbf{w}_1 + \mathbf{w}_2) \cdot \mathbf{e},$$

where \mathbf{e} is the direction vector of the edge.

7.2. A preconditioner for $\mathbf{H}(\text{div}, \Omega)$ -elliptic problems. In this case the decomposition (6.5) provides the starting point. It suggests that we choose the following auxiliary spaces:

1. $W_1 := S_h$ with inner product $\bar{a}_1(\Psi_h, \Psi_h) := \|\Psi_h\|_{H^1(\Omega)}^2 + \tau \|\Psi_h\|_{L^2(\Omega)}^2$, which is suggested by (6.6) and (6.11). The corresponding transfer operator is $\Pi_1 := \Pi_h^{\text{div}}$ and, thanks to (4.11), (2.11) holds with constant c_1 depending only on the shape regularity of the mesh. The related interpolation matrix \mathbf{P}_{div} assigns to each face of the mesh with unit normal \mathbf{n} and area $|F|$ the number

$$(7.5) \quad \frac{1}{3}|F|(\mathbf{w}_1 + \mathbf{w}_2 + \mathbf{w}_3) \cdot \mathbf{n},$$

where \mathbf{w}_i is the vectorial nodal value at vertex i of the face.

2. $W_2 := V_h(\mathbf{curl})$ endowed with the localized inner product

$$(7.6) \quad \bar{a}_2(\mathbf{w}_h, \mathbf{w}_h) := \tau \sum_{\mathbf{q} \in \mathcal{B}(\mathbf{curl})} \|\mathbf{curl} \mathbf{w}_q\|_{L^2(\Omega)}^2, \quad \sum_{\mathbf{q} \in \mathcal{B}(\mathbf{curl})} \mathbf{w}_q = \mathbf{w}_h$$

for $\mathbf{w}_h \in V_h(\mathbf{curl})$. Evidently, the Galerkin discretization of \bar{a}_2 leads to a diagonal matrix denoted by $\mathbf{D}_{\mathbf{curl}}$. A closer inspection of $\mathcal{B}(\mathbf{curl})$ verifies that $\mathbf{D}_{\mathbf{curl}}$ can never be singular.

The transfer operator associated with W_2 is $\mathbf{curl} : V_h(\mathbf{curl}) \mapsto V_h(\text{div})$ and $c_2 = 1$ is obvious. Its matrix representation \mathbf{C} coincides with the incidence matrix of (interior) edges and faces of the mesh; see [21, section 3.1].

3. $W_3 := S_h$ with norm $\sqrt{\tau} \|\cdot\|_{H^1(\Omega)}$ (cf. (6.6) and (6.11)) and transfer operator $\mathbf{curl} : S_h \mapsto V_h(\text{D})$. Again, we immediately get $c_3 = 1$ for the constant from (2.11). Owing to the commuting diagram property (4.6) and (4.9), the matrix associated with this transfer is given by $\mathbf{CP}_{\mathbf{curl}}$.

Summing up, the matrix representation of the auxiliary space preconditioner for the variational problem (1.2) discretized on $V_h(\text{div})$ is given by

$$(7.7) \quad \mathbf{B}_{\text{div}} := \mathbf{D}_A^{-1} + \mathbf{P}_{\text{div}}(\mathbf{L} + \tau \mathbf{M})^{-1} \mathbf{P}_{\text{div}}^T + \mathbf{CD}_{\mathbf{curl}}^{-1} \mathbf{C}^T + \tau^{-1} \mathbf{CP}_{\mathbf{curl}}(\mathbf{L} + \tau \mathbf{M})^{-1} \mathbf{P}_{\mathbf{curl}}^T \mathbf{C}^T.$$

All transfer operators are purely local.

THEOREM 7.2. *For $0 < \tau \leq 1$ the spectral condition number $\kappa(\mathbf{B}_{\text{div}} \mathbf{A}_{\text{div}})$ depends only on Ω and the shape regularity of the mesh.*

In the 2-regular case $\kappa(\mathbf{B}_{\text{div}} \mathbf{A}_{\text{div}})$ is bounded independently of τ , but the quasi-uniformity of the mesh may affect the bound.

Proof. We merely need to appeal to (6.6), (6.11), and (2.14), because good bounds for c_1, c_2, c_3 , and c_s follow from the above arguments. \square

Remark 9. If boundary conditions are imposed on $\mathcal{H}(\text{D}, \Omega)$, the auxiliary space S_h should be chosen differently in the 2-regular case: it should comprise piecewise linear continuous vector fields, for which merely the tangential or normal components, respectively, vanish on $\partial\Omega$. Of course, this choice can be made in any case, because enlarging the auxiliary space will not affect the estimates adversely unless the continuity of Π is destroyed. On the other hand, tangential boundary conditions are awkward in terms of implementation; cf. the discussion in [5, section 5]. Moreover, as stressed in Remark 8, there is absolutely no numerical evidence that total zero boundary conditions for S_h do any harm.

7.3. Applications to problems with variable coefficients. So far we have skirted the case of variable coefficients, for instance, when we encounter the bilinear form

$$(7.8) \quad a(\mathbf{u}, \mathbf{v}) := (\alpha \operatorname{curl} \mathbf{u}, \operatorname{curl} \mathbf{v})_0 + (\beta \mathbf{u}, \mathbf{v})_0, \quad \mathbf{u}, \mathbf{v} \in \mathbf{H}_0(\operatorname{curl}, \Omega),$$

with coefficient functions $\alpha, \beta \in L^\infty(\Omega)$, because the current theory fails to give any useful information about how strong variations of α and β affect the quality of the nodal auxiliary space preconditioners.

We can give only a heuristic recipe for how the algorithms may be adapted to the general bilinear form from (7.8). The idea is that the coefficient α will be used to define the matrix \mathbf{L} in (7.3). This means that \mathbf{L} agrees with the Galerkin matrix of the bilinear form $(\mathbf{u}, \mathbf{v}) \mapsto (\alpha \operatorname{grad} \mathbf{u}, \operatorname{grad} \mathbf{v})_0$ on \mathcal{H}^1 . The coefficient β enters the matrices \mathbf{M} and Δ ; that is, they represent $(\mathbf{u}, \mathbf{v}) \mapsto (\beta \mathbf{u}, \mathbf{v})_0$ and $(\varphi, \psi) \mapsto (\beta \operatorname{grad} \varphi, \operatorname{grad} \psi)_0$ on \mathcal{H}^1 and $V_h(\operatorname{grad})$, respectively. Note that τ is now incorporated into the coefficient β .

8. Numerical experiments. The theory makes a statement about the asymptotic behavior of the nodal auxiliary, but information about concrete condition numbers remains hidden in several elusive constants. In this section we wish to demonstrate that the preconditioner actually achieves reasonably small condition numbers for relevant model problems. Moreover, we monitor the impact of the relative scaling of both parts of the bilinear form $a(\cdot, \cdot)$ from (1.3). Reaching beyond the scope of the theory, we will also examine the impact of strongly varying coefficients in (7.8). Throughout, nodal auxiliary spaces with zero boundary values for all vector components will be used (“generic case”).

The first series of experiments is conducted in two dimensions. Note that in two dimensions the operators div and curl acting on vector fields merely differ by a rotation of $\frac{\pi}{2}$. Therefore, both variational problems (1.1) and (1.2) are covered when we consider the bilinear form

$$(8.1) \quad a(\mathbf{u}, \mathbf{v}) := (\operatorname{curl} \mathbf{u}, \operatorname{curl} \mathbf{v})_0 + \tau (\mathbf{u}, \mathbf{v})_0, \quad \mathbf{u}, \mathbf{v} \in \mathbf{H}_0(\operatorname{curl}, \Omega),$$

where curl is the scalar-valued two-dimensional rotation $\operatorname{curl} \mathbf{u} = \frac{\partial u_1}{\partial x_2} - \frac{\partial u_2}{\partial x_1}$.

In two dimensions we can study the asymptotics with manageable computational effort. We emphasize that all the considerations underlying the nodal auxiliary subspace approach in three dimensions carry over to (8.1): Galerkin discretization can be based on edge elements on triangular meshes, for which curl-free functions can be represented as gradients of piecewise linear Lagrangian finite element functions.

In most experiments we used the preconditioner given by the two-dimensional counterpart of (7.3). A direct solver was employed to realize the multiplications with the inverse matrices. Extremal eigenvalues were computed by means of a Lanczos procedure up to an accuracy of at least two digits.

Experiment I. A sequence of meshes of two polygonal domains was created by the regular refinement of the coarse meshes depicted in Figure 8.1. One domain is convex, that is, it satisfies the assumptions of the 2-regular case, while the other fails to do so. Spectral condition numbers of $\mathbf{B}_{\operatorname{curl}} \mathbf{A}_{\operatorname{curl}}$, $\mathbf{A}_{\operatorname{curl}}$ the edge element Galerkin matrix related to (8.1), were computed for different choices of τ ; see Tables 8.1 and 8.3. A variant of the preconditioner relying on two steps of Gauss–Seidel smoothing (see section 2) was tested in the same setting. The measured condition numbers are listed in Tables 8.5 and 8.6.

We also keep track of the number of PCG iterations required to solve the discrete variational problems with bilinear form $a(\cdot, \cdot)$ from (8.1) and constant vector field $\mathbf{f} = \begin{pmatrix} 1 \\ 1 \end{pmatrix}$ as the right-hand side. A relative reduction of the Euclidean norm of the residual vector by a factor of 10^6 was used as termination criterion. The results are recorded in Tables 8.2 and 8.4.

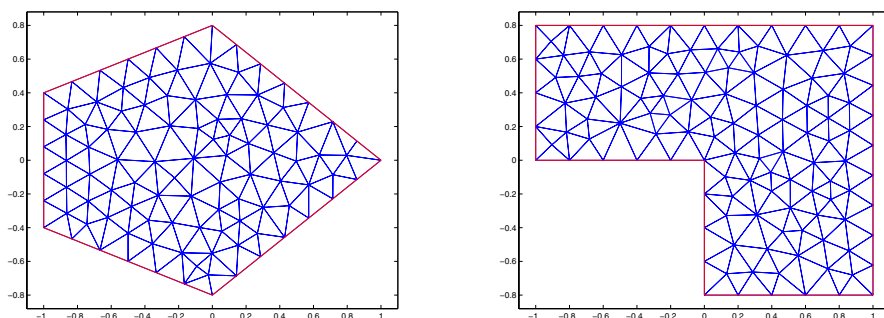


FIG. 8.1. Coarsest meshes used in Experiment I.

TABLE 8.1
Condition numbers for Experiment I: Convex polygon.

Level	# cells	τ								
		10^{-4}	10^{-3}	10^{-2}	10^{-1}	1	10	10^2	10^3	10^4
0	171	20.4	20.4	20.3	20.1	18.2	11.7	5.0	2.6	3.7
1	684	25.0	25.0	25.0	24.7	23.0	16.5	8.3	3.6	3.3
2	2736	28.4	28.4	28.4	28.2	26.6	20.8	12.5	6.2	2.9
3	10944	31.2	31.2	31.2	31.0	29.7	24.8	17.5	9.3	4.6
4	43776	33.5	33.5	33.5	33.3	32.2	28.3	22.1	14.2	7.1
5	175104	35.2	35.2	35.2	35.1	34.2	31.1	26.1	19.1	11.0

TABLE 8.2
Required PCG iterations for Experiment I: Convex polygon.

Level	# cells	τ								
		10^{-4}	10^{-3}	10^{-2}	10^{-1}	1	10	10^2	10^3	10^4
0	171	29	29	29	28	27	24	15	9	11
1	684	33	33	33	33	32	28	20	11	11
2	2736	36	36	36	36	35	31	25	16	10
3	10944	38	38	39	38	38	34	29	20	13
4	43776	41	41	41	41	40	37	32	25	17
5	175104	42	42	43	42	42	39	34	28	21

The condition numbers hardly deteriorate on successively finer meshes. The slight dependence on the refinement level is a commonly observed preasymptotic phenomenon; cf. Remark 2 in [8]. A similar statement applies to the number of CG iterations. Robustness in τ is evident though not covered by theory when using a nodal auxiliary space with zero boundary conditions (“generic setting,” Table 3.1). Using a Gauss–Seidel smoother instead of Jacobi improves the performance at increased costs for a single application of the preconditioner.

Experiment II. Starting from a coarse mesh on the “L-shaped domain” (Figure 8.1, right) we generate a sequence of meshes by strictly local refinement; see

TABLE 8.3
Condition numbers for Experiment I: L-shaped domain.

Level	# cells	τ								
		10^{-4}	10^{-3}	10^{-2}	10^{-1}	1	10	10^2	10^3	10^4
0	205	63.0	62.9	62.6	59.9	42.5	14.9	4.9	2.6	4.2
1	820	69.5	69.4	69.1	66.2	47.7	18.4	8.7	3.2	3.4
2	3280	71.6	71.6	71.3	68.4	49.5	19.9	12.2	5.9	2.4
3	13120	72.3	72.3	72.0	69.0	50.1	21.2	15.6	9.2	4.0
4	52480	72.5	72.5	72.2	69.2	50.3	23.4	18.9	13.0	7.0
5	209920	72.6	72.6	72.3	69.3	50.4	25.2	21.7	16.7	10.3

TABLE 8.4
Required PCG iterations for Experiment I: L-shaped domain.

Level	# cells	τ								
		10^{-4}	10^{-3}	10^{-2}	10^{-1}	1	10	10^2	10^3	10^4
0	171	35	35	35	34	33	25	15	9	12
1	684	40	40	40	40	37	30	21	11	11
2	2736	43	43	43	43	40	33	25	16	9
3	10944	46	46	46	46	44	36	28	20	12
4	43776	49	49	49	48	47	38	31	25	17
5	175104	51	51	51	51	49	41	34	28	20

TABLE 8.5
Experiment I, condition numbers on convex polygon with symmetric GS smoothing.

Level	# cells	τ								
		10^{-4}	10^{-3}	10^{-2}	10^{-1}	1	10	10^2	10^3	10^4
0	171	6.5	6.5	6.5	6.4	5.6	3.1	1.9	2.0	2.0
1	684	9.4	9.4	9.4	9.3	8.4	5.3	2.4	2.0	2.0
2	2736	11.8	11.8	11.8	11.7	10.8	7.6	3.7	2.3	2.0
3	10944	13.7	13.7	13.7	13.6	12.7	9.7	5.7	2.9	2.2
4	43776	15.2	15.2	15.2	15.1	14.4	11.8	8.0	4.2	2.7
5	175104	16.4	16.4	16.4	16.3	15.7	13.6	10.4	6.4	3.2

TABLE 8.6
Experiment I, condition numbers on L-shaped domain with symmetric GS smoothing.

Level	# cells	τ								
		10^{-4}	10^{-3}	10^{-2}	10^{-1}	1	10	10^2	10^3	10^4
0	171	19.6	19.6	19.5	18.7	13.0	4.1	1.8	2.0	2.0
1	684	28.8	28.8	28.7	27.5	19.6	6.9	2.3	2.0	2.0
2	2736	33.5	33.5	33.4	32.0	23.1	8.8	3.9	2.2	2.0
3	10944	35.3	35.3	35.1	33.7	24.4	9.7	5.7	2.7	2.1
4	43776	35.9	35.9	35.7	34.3	24.9	10.3	7.3	4.1	2.5
5	175104	36.1	36.1	36.0	34.5	25.1	11.4	9.0	6.0	3.1

Figure 8.2. As in the previous experiment we recorded spectral condition numbers $\kappa(\mathbf{B}_{\text{curl}}\mathbf{A}_{\text{curl}})$; see Figure 8.3. This time, we monitor their dependence on the smallest size h_{\min} of mesh cells.

The conclusions drawn in Experiment I carry over verbatim.

Experiment III. To study the response of the preconditioner to nonconstant coefficients, we apply it to the bilinear form

$$(8.2) \quad a(\mathbf{u}, \mathbf{v}) := (\alpha \operatorname{curl} \mathbf{u}, \operatorname{curl} \mathbf{v})_0 + \tau (\beta \mathbf{u}, \mathbf{v})_0, \quad \mathbf{u}, \mathbf{v} \in \mathbf{H}_0(\operatorname{curl}, \Omega),$$

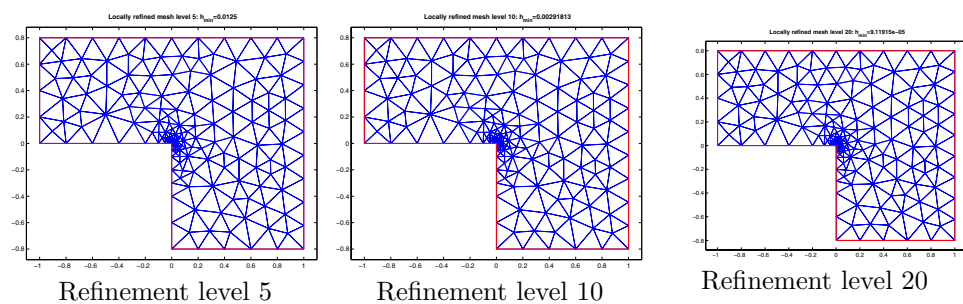


FIG. 8.2. Sequence of locally refined meshes.

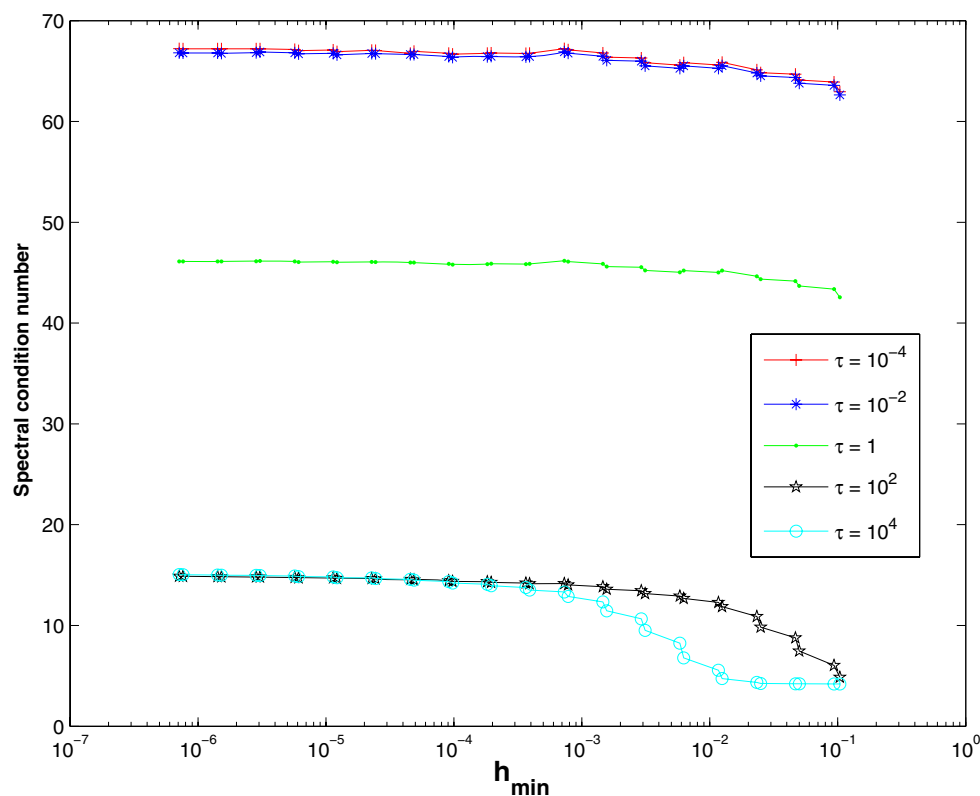


FIG. 8.3. Behavior of auxiliary space preconditioner on locally refined meshes.

with $\alpha, \beta \in L^\infty(\Omega)$. This is the two-dimensional analogue of (7.8). The implementation of the preconditioner \mathbf{B}_{curl} follows the policy outlined in section 7.3.

We consider $\Omega =]-1, 1[^2$ with a triangular subdomain Ω_1 that is resolved by the mesh; see Figure 8.4. The coefficient functions behave like

$$(8.3) \quad \alpha(\mathbf{x}) := \begin{cases} \alpha_1 & \text{if } \mathbf{x} \in \Omega_1, \\ 1 & \text{elsewhere,} \end{cases} \quad \beta(\mathbf{x}) := \begin{cases} \beta_1 & \text{if } \mathbf{x} \in \Omega_1, \\ 1 & \text{elsewhere.} \end{cases}$$

We recorded the condition numbers of the preconditioned stiffness matrices on sequences of meshes arising from successive regular refinement of the mesh depicted

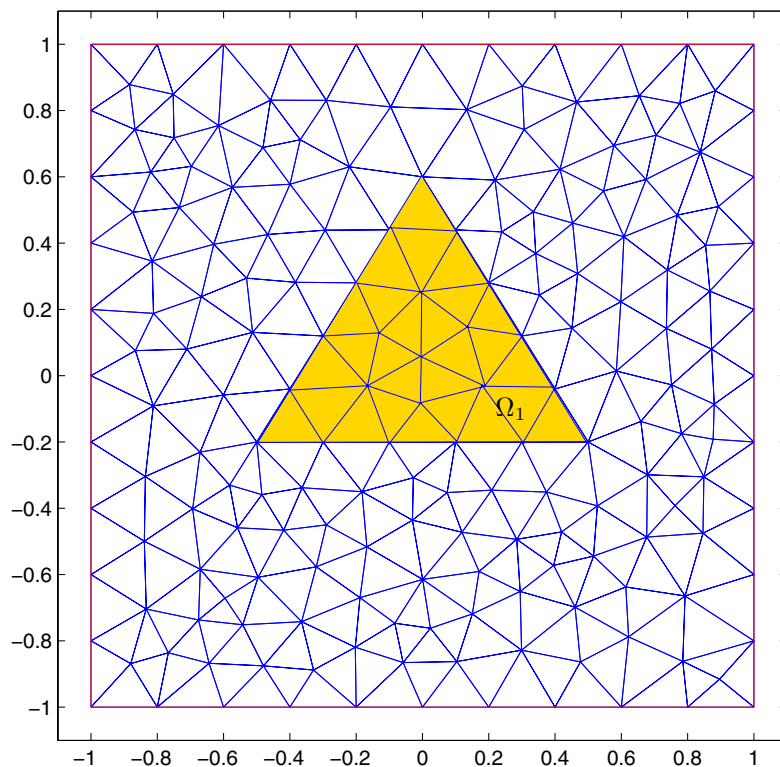


FIG. 8.4. Subdomains with piecewise constant coefficients and associated coarsest triangular mesh.

in Figure 8.4; see Tables 8.7 and 8.9. In addition, Tables 8.8 and 8.10 give the number of CG iterations required for a relative reduction of the Euclidean residual norm by a factor of 10^6 . As before, zero was used as an initial guess and we chose the source field $\mathbf{f} = \begin{pmatrix} 1 \\ 1 \end{pmatrix}$.

TABLE 8.7

Condition numbers (two digits) recorded in Experiment III: Discontinuous coefficient α , $\beta_1 = 1$.

Level	# cells	α_1										
		0.001	0.01	0.1	2	5	10	20	50	100	200	1000
0	332	19	18	16	18	21	24	28	31	33	34	35
1	1328	23	21	20	21	24	27	31	36	38	39	40
2	5312	28	27	22	23	25	29	33	37	40	41	42
3	21248	35	32	24	25	26	30	34	38	40	42	43
4	84992	41	36	26	26	27	30	34	38	41	42	43
5	339968	46	39	27	27	28	31	34	39	41	42	43

By and large, we observe that the condition number of the preconditioned system is not much affected by steep jumps in the coefficients α or β . A slight deterioration is caused by large values of β inside Ω_1 . The same holds for the convergence of the preconditioned CG iterations. It seems that the behavior of the method surpasses the predictions of the theory.

Experiment IV. In this experiment we study the auxiliary space preconditioner for genuine three-dimensional boundary value problems of the form (1.1). Zero Dirich-

TABLE 8.8
Number of CG-iterations for Experiment III: Discontinuous coefficient α , $\beta_1 = 1$.

		α_1										
Level	# cells	0.001	0.01	0.1	2	5	10	20	50	100	200	1000
0	332	33	32	28	30	31	33	34	36	36	35	37
1	1328	37	35	34	33	36	37	38	39	41	42	42
2	5312	43	42	37	37	38	41	42	44	44	45	46
3	21248	49	48	39	39	41	43	45	47	48	48	50
4	84992	54	52	41	41	42	45	48	50	51	52	53
5	339968	58	56	44	43	45	48	50	52	53	54	55

TABLE 8.9
Condition numbers (two digits) measured in Experiment III: Discontinuous coefficient β , $\alpha_1 = 1$.

		β_1										
Level	# cells	0.001	0.01	0.1	2	5	10	20	50	100	200	1000
0	332	17	17	18	18	18	20	24	32	39	48	64
1	1328	21	21	21	21	21	22	26	35	44	53	73
2	5312	23	23	23	23	23	24	27	36	46	56	78
3	21248	24	25	25	25	25	25	28	37	46	57	80
4	84992	26	26	26	26	26	27	28	37	46	57	80
5	339968	27	27	27	27	27	28	29	37	46	57	81

TABLE 8.10
Number of CG-iterations for Experiment III: Discontinuous coefficient β , $\alpha_1 = 1$.

Level	# cells	β_1										
		0.001	0.01	0.1	2	5	10	20	50	100	200	1000
0	332	30	30	30	30	30	31	33	35	38	39	41
1	1328	35	35	34	34	34	34	38	40	42	43	46
2	5312	38	38	37	37	37	36	40	43	45	47	48
3	21248	39	39	38	38	39	38	40	45	47	50	53
4	84992	41	41	40	40	40	41	42	47	49	51	55
5	339968	43	43	42	42	42	43	44	49	52	54	56

let boundary conditions are used throughout; that is, $\mathcal{H}(\mathbf{curl}, \Omega) = \mathbf{H}_0(\mathbf{curl}, \Omega)$.

We consider two different domains; one is the unit cube $\Omega = \Omega_{\square} := (0, 1)^3$, and the other is the unit ball $\Omega = \Omega_{\circ} := \{x = (x_1, x_2, x_3) \in \mathbb{R}^3 : x_1^2 + x_2^2 + x_3^2 < 1\}$. Lowest order edge elements (cf. section 4) are applied to discretize (1.1) on quasi-uniform simplicial triangulations of both domains. We apply the preconditioner $\mathbf{B}_{\mathbf{curl}}$ given in (7.3) to the discretized systems with

1. \mathbf{D}_A^{-1} replaced with the approximate inverse corresponding to three iterations of the symmetric point Gauss-Seidel method for $\mathbf{A}_{\mathbf{curl}}$,
2. $(\mathbf{L} + \tau\mathbf{M})^{-1}$ replaced with one V-cycle of an AMG method [35] for $\mathbf{L} + \tau\mathbf{M}$, and
3. $(-\Delta)^{-1}$ replaced with one V-cycle AMG method for matrix $-\Delta$ of the discrete vector Laplacian.

The matrices \mathbf{L} and \mathbf{M} correspond to the generic case; see Table 3.1.

We study the condition number of $\mathbf{B}_{\mathbf{curl}}\mathbf{A}_{\mathbf{curl}}$ on sequences of uniformly and regularly refined triangulations of both domains. On the unit cube the coarsest mesh is obtained by splitting each cell of a uniform tensor product grid into six tetrahedra. For the sphere, a mesh generator is employed to get a sequence of increasingly finer meshes, whose tetrahedra all have about the same size and little distortion. Condition number

estimates are computed by means of the Lanczos method and listed in Tables 8.11 and 8.12 for different values of the scaling parameter τ .

TABLE 8.11
Unit cube: Spectral condition numbers of $\mathbf{B}_{\text{curl}}\mathbf{A}_{\text{curl}}$.

Level	# cells	τ		
		10^{-4}	1	10^4
1	6×8^3	4.645	4.580	2.943
2	6×16^3	4.689	4.644	2.952
3	6×32^3	4.842	4.817	2.983
4	6×48^3	4.954	4.771	2.969

TABLE 8.12
Unit ball: Spectral condition numbers of $\mathbf{B}_{\text{curl}}\mathbf{A}_{\text{curl}}$.

Level	# cells	τ		
		10^{-4}	1	10^4
1	2197	2.893	2.911	3.021
2	4462	3.334	3.372	3.317
3	8865	3.280	3.288	3.430
4	17260	3.499	3.494	3.329
5	66402	3.955	3.932	3.431
6	95593	4.132	4.102	5.022
7	148554	4.497	4.246	3.513
8	242588	4.340	4.552	3.391

As before, we also record the the number of iterations required for the PCG method with the above preconditioner to reduce the \mathbf{B}_{curl} -norm of the residual by a factor of 10^6 . The iteration counts for different values of τ are given in Tables 8.13 and 8.14. In both cases a zero initial guess was used and the right-hand side was such that the corresponding exact solutions of the boundary value problems are

$$\mathbf{u}(x, y, z) = \begin{pmatrix} xyz(x-1)(y-1)(z-1) \\ \sin(\pi x) \sin(\pi y) \sin(\pi z) \\ (1-e^x)(1-e^{x-1})(1-e^y)(1-e^{y-1})(1-e^z)(1-e^{z-1}) \end{pmatrix} \text{ on } \Omega_{\square},$$

$$\mathbf{u}(x, y, z) = (x^2 + y^2 + z^2 - 1)\mathbf{1} \text{ on } \Omega_{\circ}.$$

TABLE 8.13
Number of PCG iterations on unit cube.

Level	# cells	τ								
		10^{-4}	10^{-3}	10^{-2}	10^{-1}	1	10	10^2	10^3	10^4
1	6×8^3	14	14	14	14	14	13	10	10	10
2	6×16^3	14	14	14	14	14	13	11	10	9
3	6×32^3	14	14	14	14	14	13	12	10	9
4	6×48^3	14	14	14	14	14	13	12	10	9

The observations perfectly match those made in two dimensions: the condition numbers and iteration counts are essentially independent of the meshwidth and τ . The number of PCG iterations decreases slightly when τ gets larger.

To illustrate the importance of the extra smoothings \mathbf{D}_A^{-1} in our preconditioner (7.3), we recorded the number of iterations of the corresponding PCG method with the term \mathbf{D}_A^{-1} removed from the preconditioner (7.3). The results are given in Table 8.15. We can see that the number of iterations doubles as the meshwidth gets halved.

TABLE 8.14
Number of PCG-iterations on unstructured grids in the unit ball.

Level	# cells	τ								
		10^{-4}	10^{-3}	10^{-2}	10^{-1}	1	10	10^2	10^3	10^4
1	2197	9	10	10	10	11	11	11	11	12
2	4462	10	10	11	11	11	12	11	11	12
3	8865	10	10	11	11	11	11	11	11	11
4	17260	10	11	11	11	12	12	11	10	11
5	66402	11	12	13	13	13	12	11	10	11
6	95593	11	12	13	13	13	12	12	11	12
7	148554	12	12	13	13	13	13	12	12	10
8	242588	12	13	13	14	14	13	12	11	10

TABLE 8.15
Number of PCG-iterations on the cube without smoothing.

Level	# cells	τ		
		10^{-4}	1	10^4
1	6×8^3	28	28	138
2	6×16^3	52	53	384
3	6×32^3	106	107	770
4	6×48^3	155	156	

Concluding remarks. Nodal auxiliary space preconditioning for discrete $\mathbf{H}(\text{curl}, \Omega)$ - and $\mathbf{H}(\text{div}, \Omega)$ -elliptic variational problems has a solid theoretical foundation and proves satisfactory in numerical tests. It can pave the way for applying standard AMG methods to boundary value problems discretized by means of edge or face finite elements. Numerous improvements of the method that can make use of better smoothers and refined auxiliary spaces are conceivable.

Acknowledgments. The authors wish to thank Wang Mengyu, Hangzhou University, and Patrick Meury, ETH Zürich, for writing parts of the MATLAB code for the two-dimensional experiments and also Tan Lin and Shu Shi, Xiangtan University, for their help with the three-dimensional experiments.

REFERENCES

- [1] C. AMROUCHE, C. BERNARDI, M. DAUGE, AND V. GIRAULT, *Vector potentials in three-dimensional nonsmooth domains*, Math. Methods Appl. Sci., 21 (1998), pp. 823–864.
- [2] D. ARNOLD, R. FALK, AND R. WINTHER, *Multigrid Preconditioning in $H(\text{div})$ on Non-convex Polygons*, Tech. rep., Penn State University, College Park, PA, 1997.
- [3] D. ARNOLD, R. FALK, AND R. WINTHER, *Preconditioning in $H(\text{div})$ and applications*, Math. Comp., 66 (1997), pp. 957–984.
- [4] D. ARNOLD, R. FALK, AND R. WINTHER, *Multigrid in $H(\text{div})$ and $H(\text{curl})$* , Numer. Math., 85 (2000), pp. 175–195.
- [5] R. BECK, *Algebraic Multigrid by Component Splitting for Edge Elements on Simplicial Triangulations*, Tech. rep. SC 99-40, ZIB, Berlin, Germany, 1999.
- [6] M. BIRMAN AND M. SOLOMYAK, *L_2 -theory of the Maxwell operator in arbitrary domains*, Russian Math. Surveys, 42 (1987), pp. 75–96.
- [7] P. B. BOCHEV, C. J. GARASI, J. J. HU, A. C. ROBINSON, AND R. S. TUMINARO, *An improved algebraic multigrid method for solving Maxwell's equations*, SIAM J. Sci. Comput., 25 (2003), pp. 623–642.
- [8] F. BORNEMANN, *A Sharpened Condition Number Estimate for the BPX-Preconditioner of Elliptic Finite Element Problems on Highly Non-uniform Triangulations*, Tech. rep. SC 91-9, ZIB, Berlin, Germany, 1991.

- [9] A. BOSSAVIT, *Computational Electromagnetism. Variational Formulation, Complementarity, Edge Elements*, Electromagnetism 2, Academic Press, San Diego, CA, 1998.
- [10] W. BOYSE, D. LYNCH, K. PAULSEN, AND G. MINERBO, *Nodal-based finite-element modeling of Maxwell's equations*, IEEE Trans. Antennas and Propagation, 40 (1992), pp. 642–651.
- [11] F. BREZZI AND M. FORTIN, *Mixed and Hybrid Finite Element Methods*, Springer-Verlag, New York, 1991.
- [12] A. BUFFA, M. COSTABEL, AND D. SHEEN, *On traces for $\mathbf{H}(\mathbf{curl}, \Omega)$ in Lipschitz domains*, J. Math. Anal. Appl., 276 (2002), pp. 845–867.
- [13] P. CIARLET, *The Finite Element Method for Elliptic Problems*, Stud. Math. Appl. 4, North-Holland, Amsterdam, 1978.
- [14] M. COSTABEL, *A remark on the regularity of solutions of Maxwell's equations on Lipschitz domains*, Math. Methods Appl. Sci., 12 (1990), pp. 365–368.
- [15] M. COSTABEL, *A coercive bilinear form for Maxwell's equations*, J. Math. Anal. Appl., 157 (1991), pp. 527–541.
- [16] M. COSTABEL AND M. DAUGE, *Maxwell and Lamé eigenvalues on polyhedra*, Math. Methods Appl. Sci., 22 (1999), pp. 243–258.
- [17] V. GIRAULT AND P. RAVIART, *Finite Element Methods for Navier–Stokes Equations*, Springer-Verlag, Berlin, 1986.
- [18] M. GRIEBEL AND P. OSWALD, *On the abstract theory of additive and multiplicative Schwarz algorithms*, Numer. Math., 70 (1995), pp. 163–180.
- [19] R. HIPTMAIR, *Multigrid method for Maxwell's equations*, SIAM J. Numer. Anal., 36 (1998), pp. 204–225.
- [20] R. HIPTMAIR, *Discrete Hodge operators*, Numer. Math., 90 (2001), pp. 265–289.
- [21] R. HIPTMAIR, *Finite elements in computational electromagnetism*, Acta Numer., 11 (2002), pp. 237–339.
- [22] R. HIPTMAIR, *Analysis of multilevel methods for eddy current problems*, Math. Comp., 72 (2003), pp. 1281–1303.
- [23] R. HIPTMAIR, *Coupling of finite elements and boundary elements in electromagnetic scattering*, SIAM J. Numer. Anal., 41 (2003), pp. 919–944.
- [24] R. HIPTMAIR AND A. TOSELLI, *Overlapping and multilevel Schwarz methods for vector valued elliptic problems in three dimensions*, in Parallel Solution of Partial Differential Equations, P. Bjorstad and M. Luskin, eds., IMA Vol. Math. Appl. 120, Springer-Verlag, Berlin, 1999, pp. 181–202.
- [25] R. HIPTMAIR, G. WIDMER, AND J. ZOU, *Auxiliary space preconditioning in $\mathbf{H}_0(\mathbf{curl}, \Omega)$* , Numer. Math., 103 (2006), pp. 435–459.
- [26] R. HIPTMAIR AND W.-Y. ZHENG, *Local multigrid in $\mathbf{H}(\mathbf{curl})$* , Tech. rep. 2007-03, SAM, ETH Zürich, Zürich, Switzerland, 2007.
- [27] T. KOLEV AND P. VASSILEVSKI, *Parallel H^1 -based Auxiliary Space AMG Solver for $H(\mathbf{curl})$ Problems*, Report UCRL-TR-2222763, LLNL, Livermore, CA, 2006.
- [28] T. KOLEV AND P. VASSILEVSKI, *Some Experience with a H^1 -based Auxiliary Space AMG for $H(\mathbf{curl})$ Problems*, Report UCRL-TR-221841, LLNL, Livermore, CA, 2006.
- [29] J. NÉDÉLEC, *Mixed finite elements in \mathbb{R}^3* , Numer. Math., 35 (1980), pp. 315–341.
- [30] J. NÉDÉLEC, *A new family of mixed finite elements in \mathbb{R}^3* , Numer. Math., 50 (1986), pp. 57–81.
- [31] S. NEPOMNYASCHIKH, *Decomposition and fictitious domain methods for elliptic boundary value problems*, in Proceedings of the Fifth International Symposium on Domain Decomposition Methods for Partial Differential Equations, D. Keyes, T. Chan, G. Meurant, J. Scroggs, and R. Voigt, eds., SIAM, Philadelphia, 1992, pp. 62–72.
- [32] J. PASCIAK AND J. ZHAO, *Overlapping Schwarz methods in $H(\mathbf{curl})$ on polyhedral domains*, J. Numer. Math., 10 (2002), pp. 221–234.
- [33] S. REITZINGER AND J. SCHÖBERL, *Algebraic multigrid for edge elements*, Numer. Linear Algebra Appl., 9 (2002), pp. 223–238.
- [34] L. R. SCOTT AND Z. ZHANG, *Finite element interpolation of nonsmooth functions satisfying boundary conditions*, Math. Comp., 54 (1990), pp. 483–493.
- [35] K. STÜBEN, *An Introduction to Algebraic Multigrid*, Academic Press, London, 2001, pp. 413–528.
- [36] U. TROTTEMBERG, C. OOSTERLEE, AND A. SCHÜLLER, *Multigrid*, Academic Press, London, 2000.
- [37] J. XU, *Iterative methods by space decomposition and subspace correction*, SIAM Rev., 34 (1992), pp. 581–613.
- [38] J. XU, *The auxiliary space method and optimal multigrid preconditioning techniques for unstructured grids*, Computing, 56 (1996), pp. 215–235.